UNIVERSITY OF OKLAHOMA

GRADUATE COLLEGE

RESOLVING DNA USING A BARE OPEN NARROW CAPILLARY WITHOUT SIEVING MATRIX

A DISSERTATION

SUBMITTED TO THE GRADUATE FACULTY

in partial fulfillment of the requirements for the

Degree of

DOCTOR OF PHILOSOPHY

By

ZAI-FANG ZHU
Norman, Oklahoma
2014

RESOLVING DNA USING A BARE OPEN NARROW CAPILLARY
WITHOUT SIEVING MATRIX

A DISSERTATION APPROVED FOR THE
DEPARTMENT OF CHEMISTRY AND BIOCHEMISTRY

BY

_____
Dr. Shaorong Liu, Chair

_____
Dr. George Richter-Addo

_____
Dr. Robert White

_____
Dr. Rui Yang

_____
Dr. Zhibo Yang

Acknowledgments

I would like to begin by thanking my advisor, Dr. Shaorong Liu, for all your help in the past five years. Without your support and guidance, I would not have finished my Ph.D studies here at OU. Your mentoring helped me to become not only a better researcher but also a better person. Thank you many times for providing the opportunity to learn from you, and I hope the lessons will continue in the rest of my life.

I also would like to thank Dr. George Richter-Addo, Dr. Robert White, Dr. Rui Yang, and Dr. Zhibo Yang for being in my advisory committee. Your kind help and guidance are greatly appreciated.

Special thanks go to Ms. Joann Lu. By discussing questions, instructing experiments, and giving advices, you helped me through my years in Dr. Liu's group. I have been enjoying the time working with you.

I would like to thank all the members present and past in Dr. Liu's group: Dr. Guanbin Li, Dr. Chiyang He, Dr. Xiayan Wang, Xin Jiang, Jonathan Roberts, Dr. Wei Wang, Joe Sampson, Dr. Congying Gu, Huang Chen, Apeng Chen, Kyle Lynch, Dr, Ruibo Li, Dr. Lei Zhou, Dr. Haiqing

Yu, Dr, Xiaochun Wang, and Mitchell Weaver. Without your help, my research could not be accomplished.

I also would like to express my sincere gratitude to Dr. Qiaosheng Pu in Lanzhou University, PR China. Your recommendation made me join this group, and the training I got in the past five year was the best. The conversations we have had over the years aided in the advancement of my research.

I would like to thank my parents and my sisters for your love and support during my study in US. To my son Erik, I hope that you are happy and healthy, and that you become a better person than I am. Finally, I want to dedicate this dissertation to my lovely wife Yan for your love, support, and sacrifices made to help me to complete this dissertation. I am lucky to have you in my life.

Table of Contents

List of Figures

Abstract

DNA molecules encode the hereditary information utilized in all living organisms, including humans. Separating DNA fragments is essential in biological research because it informs us how DNA molecules work and eventually guides us to solve related problems based on DNA examinations. Agarose gel electrophoresis (AGE) and capillary gel electrophoresis (CGE) are the two most-widely used techniques for DNA separations. While these two techniques are capable of resolving DNA fragments nicely and efficiently, the use of viscous gels results in many issues, such as time-consuming gel preparation and tedious operations. To address these issues, our group recently developed a technique for gel-free DNA separations. As this technique was carried out in a bare narrow capillary and separations were majorly based on hydrodynamic chromatography, it was named Bare Narrow Capillary-Hydrodynamic Chromatography (BaNC-HDC). The objective of this dissertation is to develop a miniature and automatic BaNC-HDC system for rapid and high-throughput DNA separations without using any sieving matrix.

We first proposed a new configuration of electroosmotic pumps (EOPs). In this new configuration, a basic EOP unit was composed of a +EOP and a –EOP. The pump capillaries used in +EOP were derivatized

and the inner surface was positively charged. In –EOP, bare capillaries were used and the inner surface was negatively charged. In practice, high voltage was applied to the junction of +EOP and –EOP while both the inlet and outlet were grounded. With this configuration, we stacked ten open-capillary EOP units in series to boost the pressure, and a pumping pressure of up to 21.4 MPa was achieved. The performance of the constructed ten-unit EOP was evaluated by applying it to drive high performance liquid chromatography for separations of peptides or proteins.

We then explored the resolving power of BaNC-HDC and presented the extremely high efficiency of BaNC-HDC for DNA separations. By manipulating the elution velocity, efficiency of more than one million theoretical plates per meter was easily obtained. Through studying the relationship between the elution velocity and the height equivalent to a theoretical plate, we revealed the unique behaviors of BaNC-HDC in van Deemter curves. The effect of temperature on DNA separations in BaNC-HDC was also investigated.

In order to automate injections in BaNC-HDC, a microfabricated chip injector was developed. The chip injector was composed of an on-chip cross and an off-chip six-port valve, and it was able to deliver picoliters of sample

reliably and reproducibly. By integrating this chip injector and the developed EOP into the BaNC-HDC system, the separation of GeneRuler^{TM} 1-kbp plus DNA ladder was accomplished within five minutes and plasmid DNA was accurately sized.

To improve throughput in BaNC-HDC, a splitting-based chip injector was developed. With the new injector, injections could be performed while the separation was in process, and this facilitated successive injections in BaNC-HDC. Throughput of BaNC-HDC was improved from six to fifteen samples per hour. Additionally, the injected volume can be precisely controlled at the subpicoliter level, and, for large DNA fragments, only molecules of DNA were required for each assay. The developed system was successfully applied to sizing digested λ-DNA, and all six fragments were identified within ten minutes. We also utilized the system to investigate the genetic diversity of *Saccharomyces cerevisiae* (*S. cerevisiae*) strains with short tandem repeats as markers. Short tandem repeats from two yeast strains, BG-1 and CAT-1, were resolved and distinguished within ten minutes.

Chapter 1: Introduction

1.1 Background

Separation is the core of Analytical Chemistry and most existing separation techniques are based on chromatography. Hydrodynamic chromatography (HDC) is a chromatographic technique introduced in the late 1960s by DiMarzio and Guttman,[1] and it was first termed separation by flow. In 1974, Small[2] experimentally studied the effect of column packing (bead size and type) and the ionic strength of the eluent on particle separations in HDC and also proposed the separation mechanism. Colloidal particles in the range of 500 – 1099 nm in diameter were successfully separated in Small's work. HDC has shown potential in numerous applications[3-6] and recently it found applications in DNA analysis due to the development of narrow-capillary (1 – 20 μm i.d.) HDC.[7-11]

In HDC, separations are performed in an open tube or a packed column. In an open tube, as a pressure is applied, the parabolic flow is induced. The flow streamlines near the walls of the tube are the smallest while those in the middle of the tube are the greatest. Larger particles cannot travel as closely to the wall of the tube as smaller ones do, therefore larger particles spend more time in the center of the parabolic flow than

smaller ones. This results in larger particles migrating through the tube with a higher average velocity. In HDC, these processes cause larger analytes to elute from the separation column earlier than smaller ones. In a packed column, the interstitial medium can be considered as a bundle of open tubes and the separation principle is the same as in an open tube.

Recently, our group developed a technique to resolve DNA fragments. Since this technique was based on HDC and it was performed in a bare narrow capillary, we called it Bare Narrow Capillary-HDC (BaNC-HDC).[7,8] BaNC-HDC was proved to be an excellent alternative to agarose gel electrophoresis (AGE) or capillary gel electrophoresis (CGE) for DNA separations[3,7-9,12] However, the major issue related to the extremely narrow capillary (1 – 10 μm i.d.) is that the required pressure is much higher (up to 28 MPa) while the required flow rate is greatly lower (hundreds of pL/min) than in regular HDC. Micro-pumps, especially electroosmotic pumps (EOPs), are perfectly suited to this situation. Another issue resulting from the decreased capillary i.d. is that the required sample volume significantly decreases (down to the picoliter level) and, as a result, injecting DNA samples into the narrow capillary turns out to be challenging. In this dissertation, we addressed the above-mentioned issues. The ultimate goal is to develop a miniature and automatic BaNC-HDC system for rapid and high-throughput DNA separations in free solutions.

1.2 Electroosmotic pumps (EOPs)

In this dissertation, a new EOP configuration was developed to boost the pressure output, and the developed EOPs were used to drive HPLC separations and also utilized to drive narrow-capillary HDC for DNA separations.

1.2.1 Electroosmotic flow (EOF)

EOPs are based on electroosmotic flow (EOF), which is the movement of a fluid relative to the charged surface of a solid under the influence of an electric field. In the case of a fused silica capillary, the surface is negatively charged at pH above ~3 due to the ionization of silanol groups. As shown in Figure 1.1, the negative charges attract cations from the solution filled in the capillary and a layer of cations is formed next to the capillary wall. This layer is rigidly held by the negatively charge surface, and it is named Inner Helmholtz Plane (IHP). The positive charges on IHP are not adequate to neutralize the negative charges on the surface. Thus more cations are attracted, and another layer is formed. However, the second layer is further away from the negatively charged surface and it is not rigidly held, so it tends to diffuse into the solution and is called the diffuse layer. When an electric field is applied, the diffuse layer migrates while IHP is stationary. Because the hydrated cations are relatively large,

their migration drives the bulk solution to migrate through the capillary and the movement of the bulk solution is called EOF.

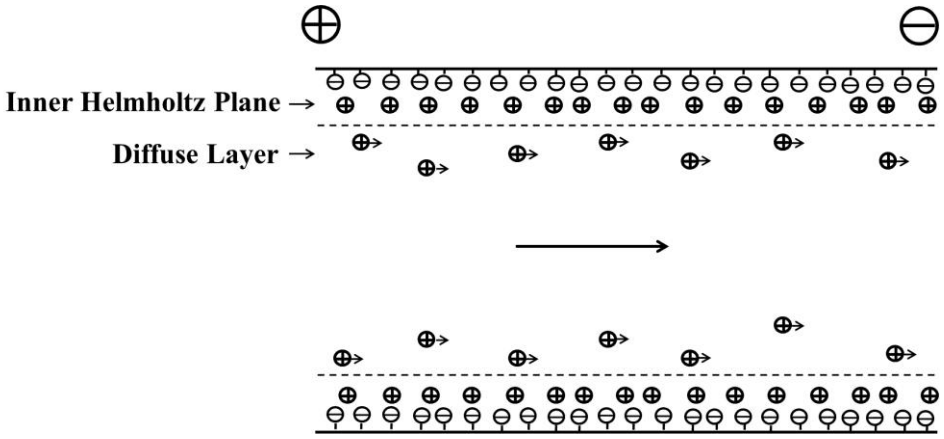

Figure 1.1. Schematic diagram of electroosmotic flow in a fused silica capillary

Compared with the parabolic flow (see Figure 1.2A) which is induced by a pressure, the flow profile of EOF is relatively flat (see Figure 1.2B). The flat flow profile reduces band broadening caused by varying velocity and this helps to considerably improve separation efficiencies in capillary electrophoresis. EOPs majorly benefit from the large velocity of EOF.

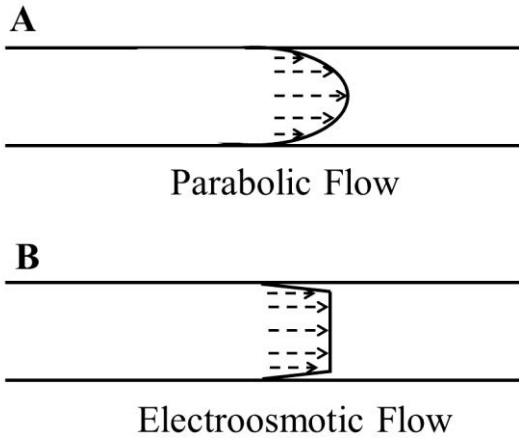

Figure 1.2. Flow profiles of electroosmotic and parabolic flow.

1.2.2 Open-capillary EOPs

Based on above-discussed EOF in a capillary, open-capillary EOPs can be fabricated. The velocity of EOF is expressed by

$$u_{eo} = \mu_{eo} * E \qquad (1.4)$$

where E is the applied electric field. μ_{eo} is electroosmotic mobility, which is determined by

$$\mu_{eo} = \frac{\epsilon\zeta}{4\pi\eta} \qquad (1.5)$$

where ε is the dielectric constant, η *is* viscosity of the solution filled in the capillary, and ζ is the zeta potential.

If the EOP is completely open, the maximum flow rate, Q_{max}, through the capillary is obtained. It is proportional to the velocity of EOF and can be written as

$$Q_{max} = \pi r^2 \mu_{eo} E \qquad (1.6)$$

where *r* is the radius of the capillary. In this case, the pressure output is zero.

If the EOP is blocked, a backward pressure, ΔP_b, is needed. This pressure generates a flow which completely offsets EOF and, based on Hagen – Poiseuille Law, it is

$$\Delta P_b = \frac{8\eta L}{\pi r^4} Q_{max} \qquad (1.7)$$

where *L* is the length of the pump capillary. In this case, the flow rate through the capillary is zero and the maximum pressure ($\Delta P_{max} = \Delta P_b$) is obtained.

Under normal working conditions, a column is connected to the EOP and the flow rate is partially offset. In this case, neither the flow rate (Q) nor the pressure output (ΔP) is zero, and they are related to each other as follows,

$$\Delta \mathrm{P} = \frac{8\eta L}{\pi r^4} (Q_{max} - Q)$$

$$= \frac{\Delta \mathrm{P}_{max}}{Q_{max}} (Q_{max} - Q)$$

$$= \Delta \mathrm{P}_{max} - \frac{\Delta \mathrm{P}_{max}}{Q_{max}} Q \qquad (1.8)$$

This relationship is visualized as in Figure 1.3. In actual practice, the pressure output can be conveniently adjusted by tuning the applied electric field, which shifts the straight line in Figure 1.3 up or down.

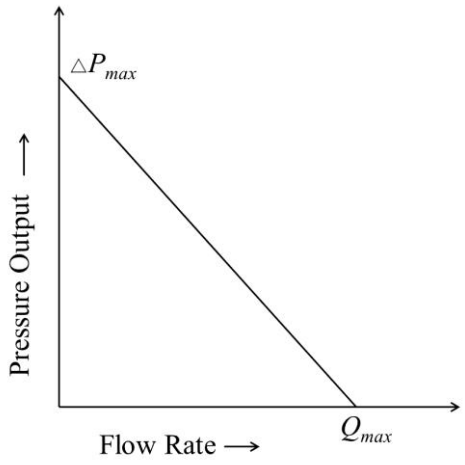

Figure 1.3. Relationship between the pressure output and the flow rate in EOPs.

In the 1990s, Liu and Dasgupta first utilized open-capillary EOPs to drive flow injection analysis. Researchers also fabricated chip-based EOPs in open channels for micro-analysis.[13-16] In that case, the pumps were called open-channel EOPs, but the working principle was the same as in open

capillaries. However, open-capillary/channel EOPs were rarely used in HPLC because the pressure output is too low.

One way to increase the pumping pressure is to cascade many EOP units in series. However, EOP units were not able to be directly connected together because the potential at the outlet of one unit is not the same as the potential at the inlet of next unit. To solve this problem, Takamura et al.[17] integrated wide channels between two EOP units (see Figure 1.4). These integrated channels could avoid short circuits, but they generated backward EOF and consequently pumped down the total pressure output of a cascaded EOP. Additionally, the wide channels limited the maximum electric field applied to the EOP system due to Joule heating and pressures above 100 psi were not obtained.

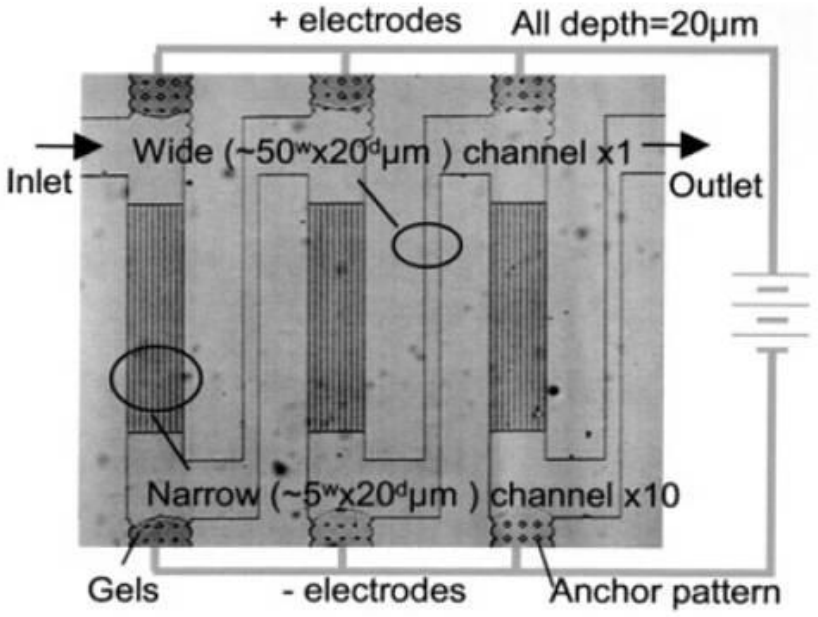

Figure 1.4. Photograph of fabricated cascade-type EOP. Reproduced from Ref. [71] with permission from John Wiley and Sons (license number: 3370341430729).

Recently, our group developed a new EOP configuration to cascade EOP units and consequently to increase the pumping pressure.[18] In this configuration, one basic EOP unit was composed of a +EOP and a –EOP. The +EOP was made with positively coated capillaries while the –EOP was fabricated with negatively coated capillaries. High voltage was applied to the junction of +EOP and -EOP while both the inlet and the outlet were grounded. EOP units could be connected together directly without short

circuits, and the maximum pressure output increased linearly as the number of EOP units increased.

In this dissertation, we detailed the procedures of fabricating this new EOP configuration. Positively coated capillaries were used to make +EOP while negatively coated capillaries were replaced with bare capillaries, which had a negatively charged surface in the pump solution (5 mM NH_4Ac, pH~6.8). With a 10-unit open-capillary EOP, a pressure of up to 21.4 MPa was obtained. To evaluate the performance the constructed 10-unit EOP, it was applied to drive high performance liquid chromatography for separations of peptides or proteins.

1.2.3 Other EOPs

Other than open capillaries/channels, packed columns, monolithic columns, and porous membrane were also used as pumping elements to construct EOPs. These pumps were categorized as packed-column, monolithic-column, and porous-membrane EOPs, respectively.

When EOPs were first introduced in 1970s by Pretorius et al.,[19] a glass column (5-cm length and 1-mm i.d.) packed with silica particles was used. Yao and Santiago[20] developed a model to predict flow rate, pressure, and thermodynamic efficiency in EOPs. Our group recently reported a monolith-based EOP which is capable of generating a pressure of up to

17,000 psi.[21] Basic units were constructed with positive and negative monolithic columns, and three basic EOP units were cascaded based on the configuration we previously described.[18] Porous membrane is usually used to make low-pressure EOPs, and the applied voltage is usually low. In 2011, Shin et al. reported a miniature EOP which was fabricated with silica membrane.[22] As the EOP was operated below 1.23 V, no O_2 or H_2 was generated in the pumping process and gas bubbles were not an issue. Instead, the electrodes, reactive Ag/Ag_2O, were consumed and a flow rate of 14.5 ± 1.5 μL/min was obtained at 0.5 V. This pump was perfectly suited to drug delivery.

In this dissertation, open-capillary EOPs were used to drive BaNC-HDC because they were stable and pump-to-pump reproducibility for pumping pressures and flow rates was satisfactory. The limited pumping pressure was an issue related to open-capillary EOPs, but it was addressed by the new EOP configuration we developed.

1.3 DNA separations

DNA molecules store the genetic information used in all living organisms. To understand how DNA molecules work, DNA separations usually need to be performed. Most DNA separations are gel-based, but gel-free DNA separations have recently shown rapid growth.

1.3.1 Gel-based DNA separations

All DNA fragments, regardless of their length, have similar charge-to-mass ratios and, as a result, they have similar electrophoretic mobility, so free-solution electrophoresis is not capable of separating DNA fragments. In gel electrophoresis, there are numerous pores within the used gel, and DNA fragments are separated based on a sieving mechanism when they migrate in the gel solution. Shorter DNA fragments pass pores easily while longer DNA fragments are obstructed by the gel, so shorter DNA fragments have larger mobilities than larger ones and they elute first.

Agarose gel electrophoresis (AGE) is the most-regularly used technique for DNA separations. Agarose gels are easy to cast and handle. Their resolving power is lower than that of polyacrylamide gels, but they are capable of separating DNA fragments in a wider range.[23-25] Standard AGE can be used to separate DNA in the range of 50 – 20, 000 bp. Beyond 20 kbp, DNA fragments move through agarose gels not depending sizes, and thus standard AGE is unable to separate them effectively.[26-28] To address the issue, Schwartz and Cantor[29] employed alternately pulsed, perpendicularly oriented electrical fields in AGE, and chromosomal DNA fragments (up to 2000 kbp) were successfully separated. This technique was latterly named pulsed-field gel electrophoresis (PFGE). Although many

alternatives have been developed, AGE, including PFGE, is the currently-accepted standard technique for DNA separations.

Capillary gel electrophoresis (CGE), also called capillary sieving electrophoresis, was introduced by Cohen and Karger[30] in the 1980s for separations of peptides or proteins. In CGE, because the capillary has larger specific area and it can dissipate Joule heating more efficiently than the slab gel, a higher electric field can be applied to achieve faster separations. Separation efficiencies can be up to 10^7 theoretical plates per meter, which are much higher than those in slab gel electrophoresis.[31,32] Additionally, CGE employed on-line detection and it is more automatic than slab gel electrophoresis.

Due to the advantages of CGE over slab gel electrophoresis, CGE has been popularly used for DNA separations. In 1988, Cohn et al.[33] first separated DNA fragments with CGE. With a capillary of 75 μm i.d. as the separation column and 7.5% crosslinked polyacrylamide gel as the sieving matrix, a DNA mixture, $(dA)_{40\text{-}60}$, was baseline separated within 8 min. As a continuation of this work, Heiger et al.[34] investigated the effect of the amount of crosslinking agent on DNA separations, and low-crosslinked or linear (zero-crosslinked) polyacrylamide gel was used. While the resolving power was comparable to that obtained with high-crosslinked polyacrylamide gel, the columns became more stable and could be used

repeatedly for longer periods of time. To improve analysis throughput, multiple capillary system, also named capillary array electrophoresis (CAE), was developed. With a 48-capillary CAE system, Mansfield et al.[35,36] analyzed microsatellite markers and 1920 samples could be processed per day.[36] 96-capillary systems were also used for simultaneous genomic typing.[37,38] CAE played the most essential role in the Human Genome Project, and CGE is the most successful alternative to slab gel electrophoresis for DNA separations.

Microchip gel electrophoresis is another powerful tool for DNA separations, and it combines the advantages of CGE and the shrunken dimension of microfluidics. In 1994, Manz and co-workers[39] reported the first application of CGE in microfabricated devices. Single-stranded DNA in the range of 10 – 25 bases was used as the model sample, and separations were accomplished within 1 min. On-chip CAE was later developed, and it was used for ultra-high-speed DNA sequencing.[40-42] In 2000, Liu et al.[43] reported automated parallel DNA sequencing in 16-channel on-chip CAE. An 8-tip pipettor was used to automatically transfer samples from a 96-well plate to the chip, and chip aligning and focusing were also automated. Currently, automatic on-chip CAE systems are commercially available for DNA separations and other analysis.

1.3.2 Gel-free DNA separations

In both AGE and CGE, viscous gels are utilized to serve as sieving matrix. However, gel preparation is usually time-consuming and loading viscous gels to a capillary or a microchannel is a tough job. Gas bubbles generated due to Joule heating is also an issue. All these problems can be automatically addressed if separations are performed in free solutions. Another drive to develop gel-free techniques is that some new techniques have better performance than gel electrophoresis in efficiency, throughput, or sample consumption.

End-labeled free-solution electrophoresis (ELFSE) is an important technique for DNA separations in free solutions, and this technique was introduced by Noolandi in the early 1990s. By attaching a charged label molecule to DNA molecules, the charge densities of DNA molecules are changed and varying electrophoretic mobilities are consequently generated. Therefore, DNA molecules can be electrophoresis-based separated in free solutions. In 1995, Volkel and Noolandi[44] experimentally investigated the electrophoresis behaviors of short single-stranded DNA in ELFSE, and DNA ranging from 5 to 50 bases was successfully separated. Heller et al.[45] first applied this technique to resolve double-stranded DNA fragments. In 2006, McCormick and Slater[46] theoretically studied the possibility to improve the resolving power of ELFSE by using electroosmotic flow. After

20+ years of development, ELFSE has become an important alternative to gel electrophoresis for DNA separations.

Other gel-free techniques include denaturing HPLC,[47] DNA prism,[48] entropic trapping,[49] and anomalous radial migration.[50] While these techniques conditionally overcame the disadvantages of gel electrophoresis, none of them resolves DNA fragments as powerfully as gel electrophoresis does. BaNC-HDC is a technique our group recently developed for gel-free DNA separations. In BaNC-HDC, a pressure is used to drive separations and a free solution is employed as the eluent. As shown in Figure 1.5A, under the influence of pressure differential, a flow is induced in a separation capillary with i.d. of *2R*. According to Hagen-Poiseuille law, the flow profile is parabolic as shown in Figure 1.5A. The flow streamlines near the capillary wall are smaller than those in the center. When two DNA fragments are injected into the separation capillary and transported under the pressure-induced flow, they migrate as particles (see Figure 1.5B). The effective radius of larger fragments, *2r*, is larger than that of smaller ones, *2r′*, ($r>r'$ as shown in Figure 1.5B). Therefore, larger fragments are not able to access the capillary as closely as smaller ones do. As a result, larger fragments remain in the center of the separation capillary and experience faster streamlines while smaller fragments experience both the faster streamlines in the center and the slower streamline near the wall. Therefore,

larger fragments move in the separation capillary with a larger average velocity than smaller ones, and they elute earlier than smaller fragments in BaNC-HDC.

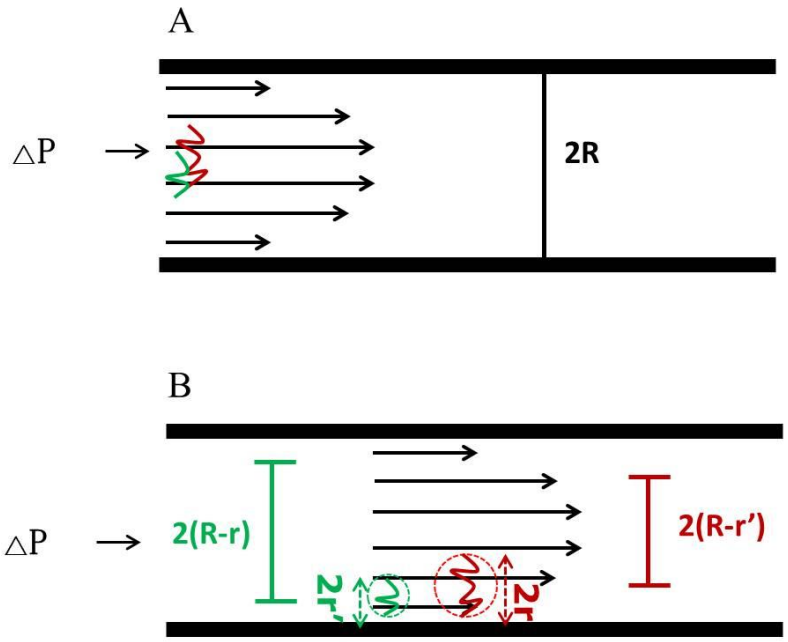

Figure 1.5. Principle of separations in BaNC-HDC.

BaNC-HDC can be used to separate DNA fragments[7,8] and proteins as well.[51] In DNA separations, fragments ranging from 75 bp to 106 kbp could be efficiently separated in a single run.[9] Efficiency of more than one million theoretical plates per meter was easily achieved,[52] and separation time was shortened to ~5 min.[53] Additionally, in BaNC-HDC, only picoliters of samples and nanoliters of eluent were consumed in each assay, and nearly zero waste was generated. Currently, laser induced fluorescence

(LIF) is solely used to monitor signal in BaNC-HDC. However, other detection techniques, such mass spectrometry and capacitively coupled contactless conductivity detection, are being examined to serve in BaNC-HDC. We expect BaNC-HDC to be established as a rapid alternative to PFGE and to play an essential role in molecular biology research.

1.4 Dissertation synopsis

The objective of this dissertation is to develop a miniature and automatic BaNC-HDC system for rapid and high-throughput DNA separation without using any sieving matrix.

In Chapter 2, a new hybrid open-capillary EOP was developed and a pumping pressure of up to 21.4 MPa was achieved. To evaluate the performance of the developed EOP, a 10-unit open-capillary EOP was constructed and it was applied to drive high performance liquid chromatography for separations of peptides or proteins

In Chapter 3, we presented the extremely high efficiency of BaNC-HDC on separating DNA fragments. By investigating the effect of the elution velocity on DNA separations, the unique behaviors of BaNC-HDC in van Deemter curves were revealed. The effect of temperature on DNA separation in BaNC-HDC was also studied.

In Chapter 4, the developed open-capillary EOP was applied to drive BaNC-HDC for gel-free DNA separations, and a microfabricated chip injector was developed for sample injections at picoliter level. While the EOP generated a flow rate and a pressure which were perfectly suited for BaNC-HDC, the chip injector was capable of injecting picoliters of DNA samples into the narrow capillary reliably and reproducibly. With the incorporated system, DNA fragments were rapidly separated with high resolutions, and, for large DNA fragments, only molecules of DNA were required for each assay. The system was finally applied to size plasmid DNA.

Chapter 5 presents a splitting-based injector for high-throughput DNA separations in BaNC-HDC. This new injection scheme allowed injecting DNA samples in BaNC-HDC at subpicoliter level. More importantly, injections could be performed while the separation was in process. This facilitated successive injections in BaNC-HDC and the throughput was consequently improved. To demonstrate the applicability of the developed BaNC-HDC system, we finally used it to simultaneously size and quantitate digested λ-DNA and short tandem repeats.

In Chapter 6, we summarize the research performed in the dissertation and provide overall conclusions. Future directions are briefly discussed.

Chapter 2: Developing High-Pressure Open-Capillary Electroosmotic Pumps

2.1 Introduction

Since being introduced in the 1970s, various types of micropumps have been developed and reviews about the progress in this field can be found in the literature.[54-56] Among all types of micropumps, electroosmotic pumps (EOPs) are receiving increasing attention because of their unique features. EOPs can generate stable pulse-free flow which is suited for microanalysis, and they can be readily integrated into lab-on-chip devices. Additionally, there are no moving parts in EOPs and the flow direction can be handily controlled.[14,54-56] In 1970s, Pretorius et al.[19] constructed the first EOPs by packing micro-particulate silica into glass columns, and the constructed EOPs were capable of driving HPLC separations. In 2000, Paul and Rakestraw[57] patented a type of EOPs which were fabricated with capillaries packed with 1 – 3 μm silica beads, and the pumps could generate a pressure of up to 5000 psi. Nie et al.[58] developed an on-chip (PMMA chip) EOP based on monolithic silica columns. Nine parallel columns were fabricated on the chip to increase the flow rate as required, and a flow rate of up to 0.6 μL/min was obtained.

In 1990s, Dasgupta and Liu developed open-capillary EOPs for microflow analysis.[59-62] With a bare capillary of 75 μm i.d. as the pump capillary, moderate pressure and flow rate were achieved for capillary electrophoresis and flow injection analysis. In 2002, Lazar and Karger[14] fabricated open-channel EOPs on chips. With the proposed pump configuration which was composed of hundreds of parallel microchannels, the flow rate was up to 400 nL/min while pressures of up to 80 psi were achieved. Achievements could also be found in other applications.[13,15,16,63] However, the limited pressure (<100 psi) generated by open-channel EOPs imposed restriction on the development of open-channel EOPs .

In 2003, Takamura et al.[17] designed a configuration to cascade EOPs. In this design, three groups of narrow channels were connected with wide channels, and voltage was in parallel applied to each channel group. Due to the existence of wide channels, the HV of the first channel group was not directly connected to the GND of the second channel group and, as a result, short circuits were avoided. The pressure output could be increased by cascading many EOP units. However, the problems associated with this design was that the wide channels limited the maximum field strength applied to the EOP system due to Joule heating and pressures above 100 psi were not obtained.

In this project, we proposed a novel configuration for constructing open-capillary EOPs. In this configuration, a basic EOP unit consists of a +EOP and a –EOP, and both the inlet and the outlet of one EOP unit were grounded. Therefore, many EOP units can be serially stacked to boost the pressure output without limit. The performance of the constructed 10-unit EOP was evaluated by applying it to drive high performance liquid chromatography (HPLC) for separations of peptides or proteins.

2.2 Experimental section

2.2.1 Chemicals and materials

Acrylamide, [N,N′-methylene bisacrylamide] (Bis), N,N,N′,N′-tetra-methylethylenediamine (TEMED), and ammonium persulfate (APS) were products of Bio-Rad Laboratories (Hercules, CA). Methacryloyloxypropyl trimethoxysilane (MPTS, 98%) was obtained from Acros (Fairlawn, NJ). p-Styrenesulfonic acid sodium salt (pSSA) was purchased from TCI (Tokyo, Japan). [2-(Methacryloyloxy)ethyl]trimethyl ammonium chloride (META, 75 wt% in water) was supplied by Sigma–Aldrich (St. Louis, MO). Stearyl methacrylate (SMA, techn.) and 2,2′-azobisisobutyronitrile (AIBN, 98%) were purchased from Aldrich (Steinheim, Germany). Cyclohexanol was supplied by J.T. Backer (Phillipsburg, NJ). Ethylene glycol dimethacrylate (EDMA, 98%) was the product of Alfa Aesar (Ward Hill, MA). 1,4-

Butanediol (99%) was obtained from Emerald BioSystems (Bainbridge Island, WA). HPLC peptide standard mixture H2016 was supplied by Sigma–Aldrich. Other chemicals were all products of Fisher Scientific International Inc. Ultrapure water purified by a Nanopure^{TM} Infinity Ultrapure Water System (Barnstead, Newton, WA) was used for preparing solutions. All fused silica capillaries were supplied by Polymicro Technologies (Phoenix, AZ).

2.2.2 EOP Configuration

In the configuration developed in this work, a basic EOP unit was composed of one +EOP and one –EOP (see Figure 2.1a). +EOPs were fabricated using coated 5 μm i.d. coated capillaries with positively charged wall while –EOPs were composed of 2 μm i.d. bare capillaries, which have negatively charged wall in the pump solution. Positive high voltage (+HV) was applied to the junction of +EOP and -EOP while both the inlet and the outlet of the EOP unit were grounded. As +HV was on, EOF drove the pump solution from the grounded inlet toward +HV in the +EOP while, in the –EOP, EOF drove the pump solution from +HV to the grounded outlet. Since both the inlet and outlet of the EOP unit were grounded, this configuration allowed us to stack EOP units in series to boost pumping power. Details on how to joint +EOP and –EOP were as shown in Figure 2.1b. Briefly, a bundle of capillaries were glued together into PEEK tubing

with epoxy. Then the peek tubing was anchored into a micro PEEK tee with a micro fitting. Two leads of the micro Tee were connected to pump/connection capillaries while the third lead was connected to a capillary filled with immobilized polyacrylamide gel. The gel-filled capillary was prepared as reported previously,[16] and it served as a salt bridge that allowed ion flow but no bulk solution flow. When high voltage was applied, bubbles were generated in the buffer reservoirs due to electrolysis, but no bubbles could migrate into the fluidic system. Therefore, the capillary filled with immobilized polyacrylamide gel was also named "bubbleless electrode". After the junction was completed, 5000 psi pressure was applied for ~24 h and no leakage was observed.

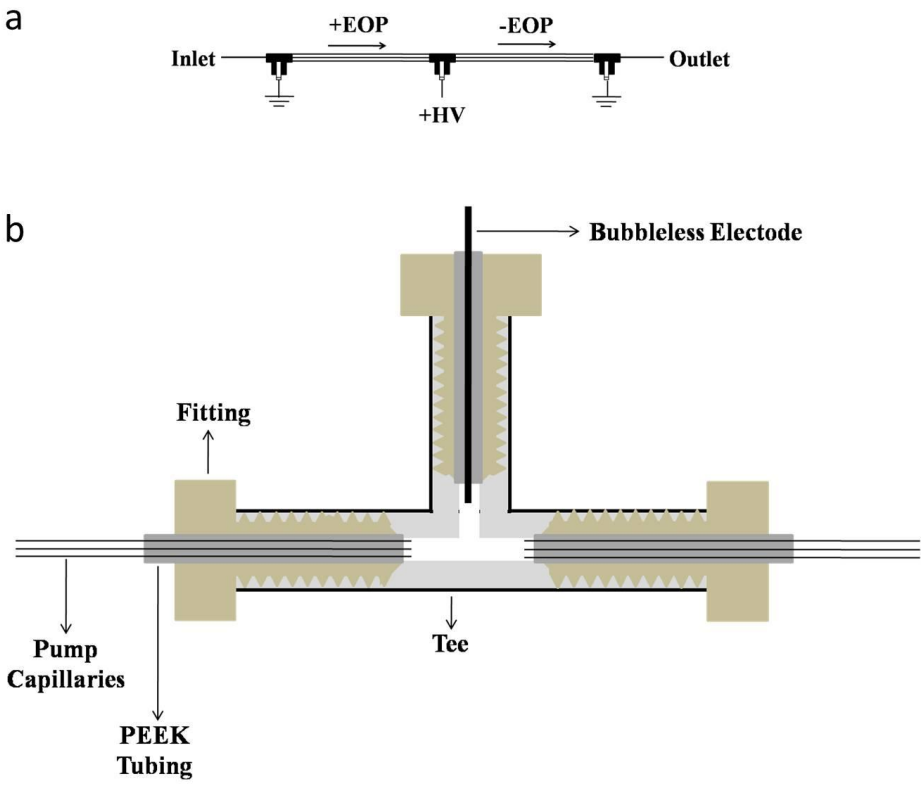

Figure 2.1. EOP configuration. (a) A basic EOP unit. +HV, positive high voltage; +EOP, fabricated using coated capillaries with positively charged wall; -EOP, fabricated using bare capillaries with negatively charged wall. (b) Schematic diagram of EOP fabrication.

2.2.3 Derivatization of pump capillaries

In this work, -EOPs were fabricated using 2 μm i.d. bare capillaries, which had negatively charged wall when filled with the pump solution (2

mM NH_4Ac, pH ~6.8). Referring back to Figure 2.1a, the electric field applied to +EOP was opposite to that applied to –EOP, so, to generate EOF with the same direction as in –EOP, capillaries utilized in +EOP need to be derivatized to make the capillary wall positively charged. The chemistry scheme used to derivatize the capillary wall was as shown in Figure 2.2. Briefly, fused capillaries of 5 μm i.d. and 150 μm o.d. were flushed with 1.0 M NaOH for 10 min at ~100 psi. The capillaries filled with 1.0 M NaOH were then sealed with rubber septa and baked in oven at 100^0C for 2 h. After being flushed with DI water and acetone at 100 psi for 20 min and 10 min, respectively, the capillaries were dried with nitrogen gas at 100 psi for 1 h. The dried capillaries were filled with 30% (v/v) MPTS, sealed with rubber septa, placed in oven at 50^0C for 14 h. The capillaries were then rinsed with acetone at 100 psi for 10 min and dried with nitrogen gas at 60 psi for 2 h. The pretreated capillaries were finally flushed with a degassed solution which was composed of 2 mL of 1.50% (w/w) META, 0.5 μL TEMED and 5 μL 10% APS in ice for 30 min, and then they were flushed with DI water at 100 psi for 20 min.

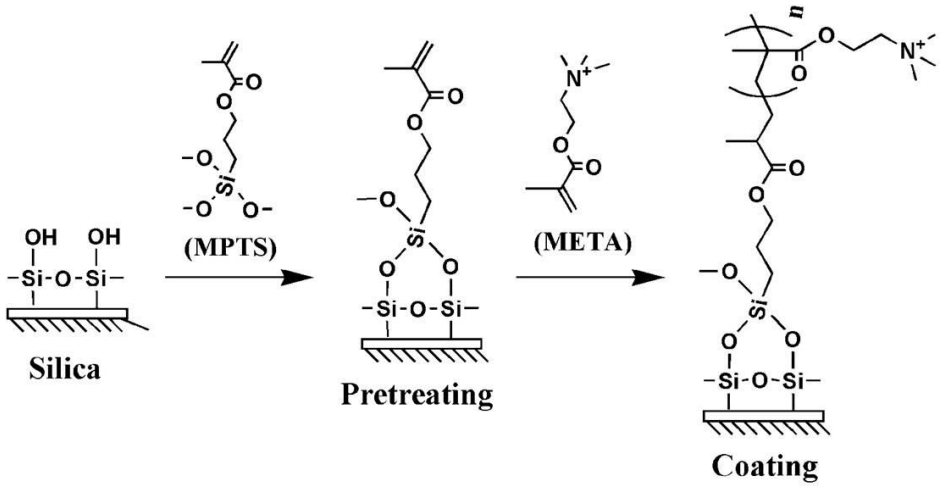

Figure 2.2. Chemistry scheme to derivatize the capillary wall for +EOPs.

2.2.4 Measurement of electroosmotic mobility

In open-capillary EOPs, both the maximum flow rate and pressure were proportional electroosmotic mobility. In this work, to measure electroosmotic mobility of pump capillaries, a capillary electrophoresis setup with a UV detector was used. At ~5 cm from the outlet of the capillary, polyimide coating was removed to form the detection window. The pump solution (2 mM NH_4Ac) was used as the running buffer and 5% (v/v) DMSO in the pump solution was injected into the capillary at 3 kV for 5 s. DMSO was detected at 210 nm, and electroosmotic mobility (μ_{eo}) was calculated as follows,

$$\mu_{eo} = \frac{l * L}{t * V} \qquad (2.1)$$

where l and L are the effective and total length of the capillary, t is the migration time of DMSO, and V is the applied voltage.

2.2.5 Measurement of maximum flow rate and pressure

Maximum flow rate and pressure are the two essential parameters characterizing EOPs. In this project, the maximum flow rate and pressure were measured before applying EOPs to HPLC separations.

An empty capillary with 200 μm i.d. was connected with a union to the outlet of EOP, and the migration of meniscus inside the empty capillary was monitored under a microscope. The maximum flow rate of EOPs, Q_{max}, was calculated with Equation 2.2,

$$Q_{max} = \frac{\pi d^2 L}{4t} \qquad (2.2)$$

where d is the inner diameter of the empty capillary, and L and t are the length and time the meniscus migrates, respectively.

The maximum pressure was measured as shown in Figure 2.3. A capillary of 10 μm i.d was connected with a union to the outlet of EOPs while the other end of the capillary was blocked with epoxy. As EOPs were on, the solution was pumped into the capillary and the air plug was

compressed. Eventually, the air plug was motionless and the maximum pressure, ΔP_{max}, was calculated using Equation 2.3,

$$\Delta P_{max} = \left(\frac{L_{total}}{L_{compressed}} - 1 \right) \times 14.7 \text{ psi} \qquad (2.3)$$

where $L_{initial}$ and L_{final} are the total length of the capillary and the length of the compressed air plug, respectively.

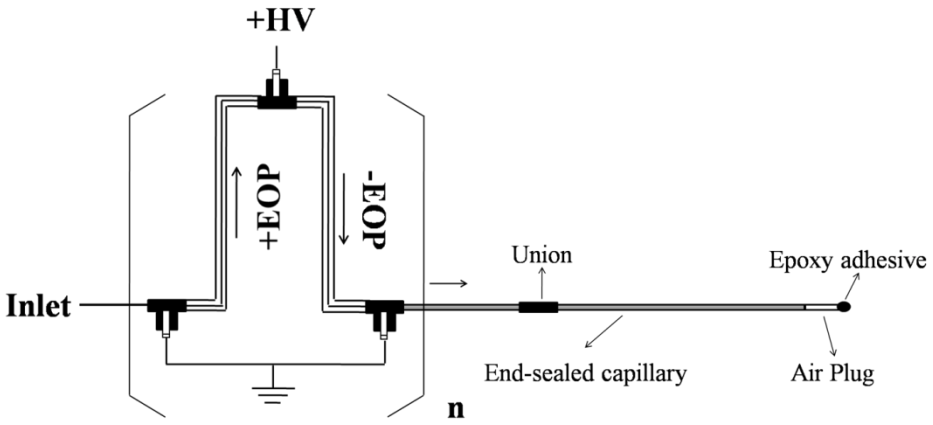

Figure 2.3. Setup for measuring the maximum pressure. *n* is the number of EOP units being stacked to boost the pump pressure.

2.2.6 Preparation of monolithic columns for HPLC separation

Monolithic columns were prepared as reported previously[64] for HPLC separations, and the protocols were as follows: (1) a 75 μm i.d. and 375 μm o.d. capillary was first pretreated with MPTS as described in Section 2.2.3;

(2) dissolved 7.5 mg AIBN in a mixture of 0.45 g OMA, 0.30 g EDMA, 0.788 g 1, 4-butanediol and 0.962 g cyclohexanol; (3) sonicated the solution for ~10 min to completely dissolve AIBN; (4) filtered the solution into a 4 mL brown bottle, degased the solution using He for ~10 min, and sonicated the solution for ~1 min to remove bubbles; (5) filled the pretreated capillary with the above solution, sealed the two ends using silicon stoppers, and kept the capillary in oven at 60^0C for ~20 h; (6) flushed the prepared column with methanol and separation buffer at 1500 psi for 3 h and 1 h, respectively.

2.2.7 An HPLC system driven by open-capillary EOPs

To evaluate applications of EOPs to driving HPLC separations, a HPLC setup driven by open-capillary EOPs was contructed as demonstrated in Figure 2.4. 10 basic EOP units were serially stacked to boost the pressure output. A 4 nL injection valve (Valco Instruments Co. Inc., Houston, TX), a capillary, and a homemade monolithic column were successively connected to the outlet EOPs. The capillary was of 200 μm i.d. and 1 m length, and it was used to contain the mobile phase for HPLC separations. A Linear UVIS 200 absorbance detector was utilized to monitor the separated analytes at 215 nm. The signal was acquired with a MCC data acquisition board (USB-1608FS, Measurement Computing Corporation, Norton, MA), and the data was processed with an in-laboratory written Labview program.

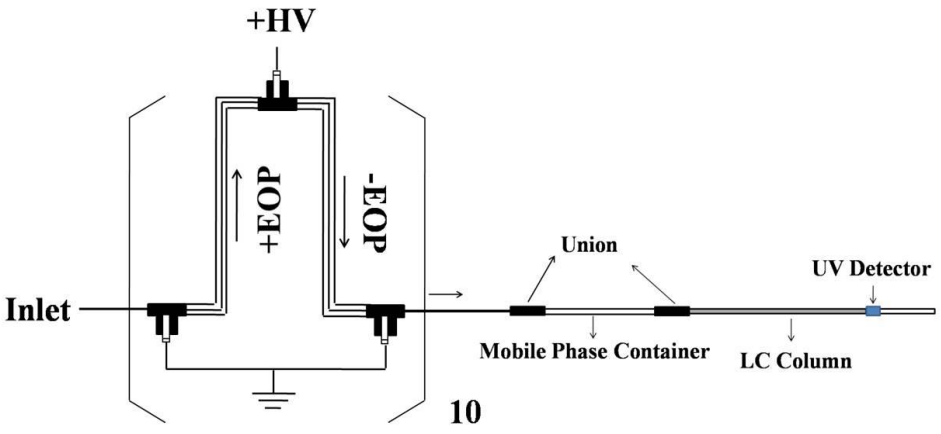

Figure 2.4. An HPLC system driven by 10-unit open-capillary EOPs. The bracket indicated 10 basic EOP units were serially stacked to boost the pressure output.

2.3 Results and discussion

In this work, we aimed to develop open-capillary EOPs which were capable of generating adequate flow rate and pressure to drive HPLC separations.

2.3.1 Characterization of bubbleless electrodes

As mentioned above, a capillary filled immobilized polyacrylamide gel was used to prevent bulk solution flow while allowing ion flow, and this

capillary was named “bubbleless electrode”. The prepared capillary was cut into small segments, and each segment had a length of 3.5 cm.

Before being used, bubbleless electrodes were soaked in the pump solution (2 mM NH_4Ac) for 24 h and the resistance was measured to estimate the voltage wasted across bubbleless electrodes. When the bubbleless electrode was of 200 μm i.d. and 3.5 cm length, the measured resistance was 29.7 MΩ. Considering that the measured resistance of the pump capillaries was $8.89*10^3$ MΩ, the voltage wasted across the bubbleless electrodes was less than 1%. Additionally, the bubbleless electrode could sustain a pressure of 5000 psi without any problem.

2.3.2 Electroosmotic mobility of pump capillaries

As reported previously,[18] the maximum flow rate (Q_{max}) and pressure (ΔP_{max}) were determined by Equations 2.4 and 2.5, respectively,

$$Q_{max} = n\pi \left(\frac{d}{2}\right)^2 \mu_{eo} \left(\frac{V}{L}\right) \qquad (2.4)$$

$$\Delta P_{max} = \frac{32\mu_{eo}\eta V}{d^2} \qquad (2.5)$$

where μ_{eo} is electroosmotic mobility, n is the number of capillaries in each EOP stage, V is the applied voltage, η is viscosity of the pump buffer, and d and L are the inner diameter and length of the pump capillaries.

Since both the maximum flow rate and pressure are proportional to electroosmotic mobility, the pH and concentration of the pump solution were optimized to increase electroosmotic mobility. As shown in Figure 2.5, as the solution pH was increased from 5.7 to 8.2, electroosmotic mobility in "+" capillaries increased while that in "-" capillaries decreased. As the pH of an NH_4Ac solution is ~6.8 and, at pH 6.8, electroosmotic mobility in both "+" and "-" capillaries was close and relatively high, an NH_4Ac solution was used as the pump solution without adjusting pH.

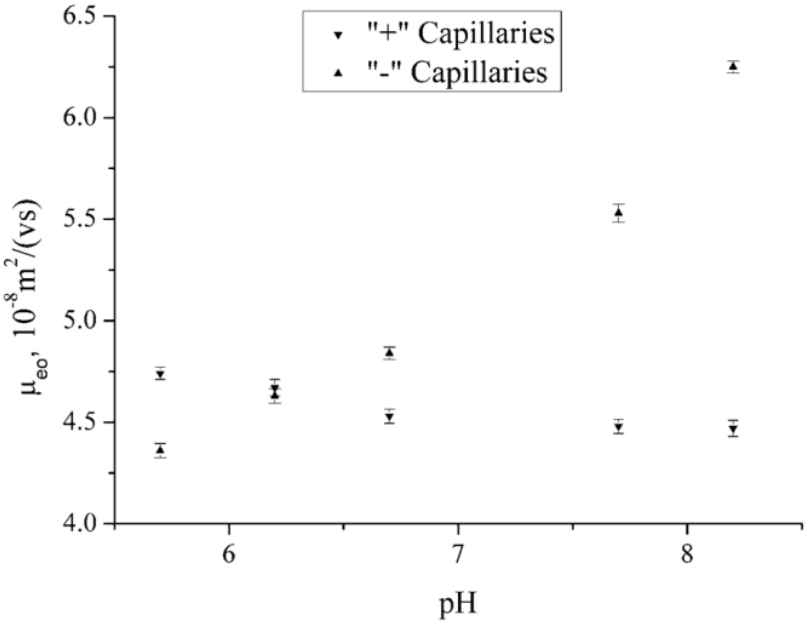

Figure 2.5. Effect of pH of the pump solution on electroosmotic mobility. pH of an NH_4Ac solution was ~6.8, and it was adjusted with concentrated

NH_4OH or HAc. The total concentration of the pump solution was controlled at 2 mM.

Effect of the concentration of the pump solution on electroosmotic mobility was also investigated. As demonstrated in Figure 2.6, decreasing the concentration from 5 mM to 0.2 mM increased electroosmotic mobility in "-"capillaries. However, when the concentration was below 2 mM, the EOP system was not stable. Therefore, 2 mM NH_4Ac was selected as the pump solution.

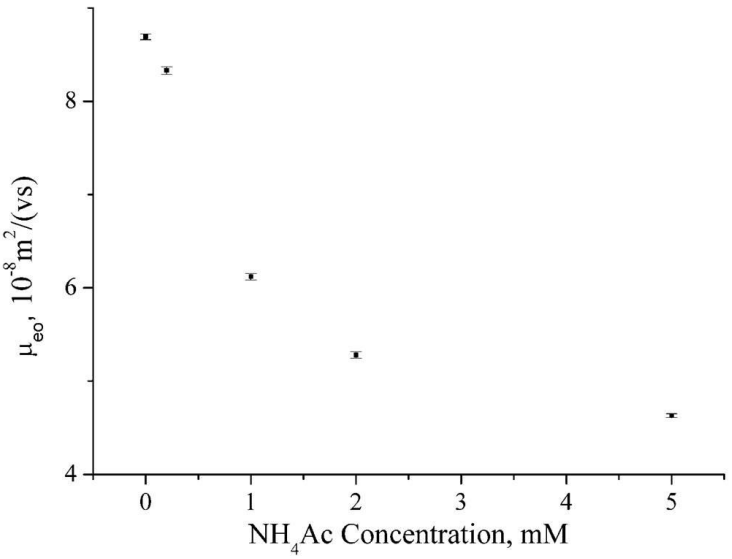

Figure 2.6. Effect of concentration of the pump solution on electroosmotic mobility. pH of the used NH_4Ac solution was not adjusted, and it was ~6.8.

2.3.3 Construction of serially stacked EOPs

Based on Equation 2.5, the maximum pressure could be drastically increased by decreasing the inner diameter of the pump capillaries. However, we ran into problems with derivatizing the capillary wall when the inner diameter was 2 μm. Therefore, 5 μm i.d. positively coated capillaries were used to construct "+" capillaries while 2 μm i.d. bare capillaries were used to make "-"EOPs. 35 capillaries were glued in each EOP stage to increase the flow rate. After the +EOP and –EOP were assembled, the maximum flow rate and pressure were measured at different applied voltage. As expected, both the maximum flow rate and pressure linearly increased with the applied voltage in the range of 5 – 25 kV. The excellent linear correlation coefficients (r^2=0.991-0.996) indicated that no excessive Joule heating was generated. We then fabricated +EOP and –EOP into a basic EOP unit as shown in Figure 2.1a and measured its maximum flow rate and pressure. While the maximum flow rate of the basic EOP unit was almost unchanged, the maximum pressure was the sum of those of +EOP and –EOP.

As mentioned above, since both the outlet and inlet of a basic EOP unit were grounded, many EOP units could be simply connected in series to increase the pressure output. As shown in Figure 2.7, the maximum pressure increased proportionally with the number of EOP units. 10-unit

open-capillary EOPs could generate a pressure of ~21.4 MPa, and the maximum flow rate was ~400 nL/min.

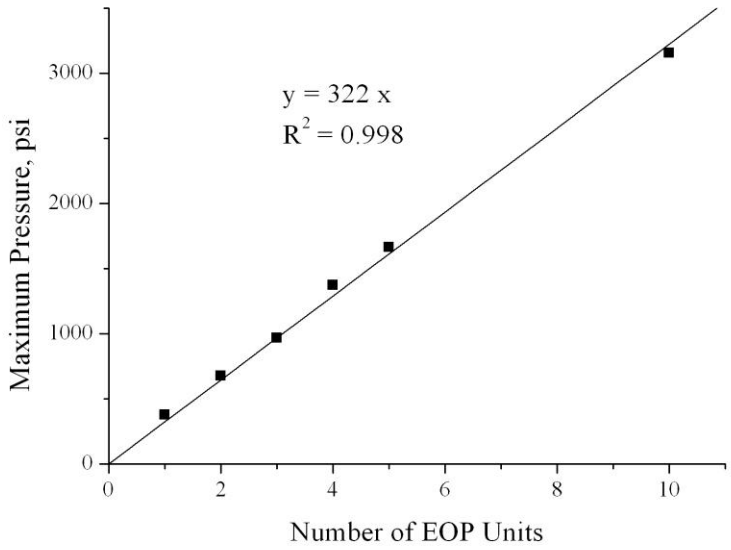

Figure 2.7. Relationship between the maximum pressure and the number of basic EOP units connected. The maximum pressure was measured as shown in Figure 2.3.

2.3.4 Applications of 10-unit open-capillary EOPs

To demonstrate applications of the pump developed in this work, we built an HPLC system as shown in Figure 2.4. The separation column was a homemade monolithic column, and the mobile phase was 15.9% (v/v)

acetonitrile and 0.1% (v/v) trifluoroacetic acid (TFA) in DI water. Because the pump solution was different from the mobile phase, a capillary of 1 m length and 200 μm i.d. was integrated between EOPs and the injection valve to contain the mobile phase for HPLC separations. A standard peptide solution containing 0.04 mg/mL Gly-Tyr (1), 0.04 mg/mL Val-Tyr- Val (2), 0.04 mg/mL Met enkephalin (3), 0.08 mg/mL Leu enkephalin, and 0.08 mg/mL Angiotension II (5) was injected, and theses five peptides were separated within 5 min (see Figure 2.8a). For protein separations, a standard solution containing 0.5 mg/mL Ribonuclease A (1), 0.8 mg/mL Insulin (2), and 1.4 mg/mL Cytochrome C was used, and these three proteins were separated within 4 min (see Figure 2.8b).

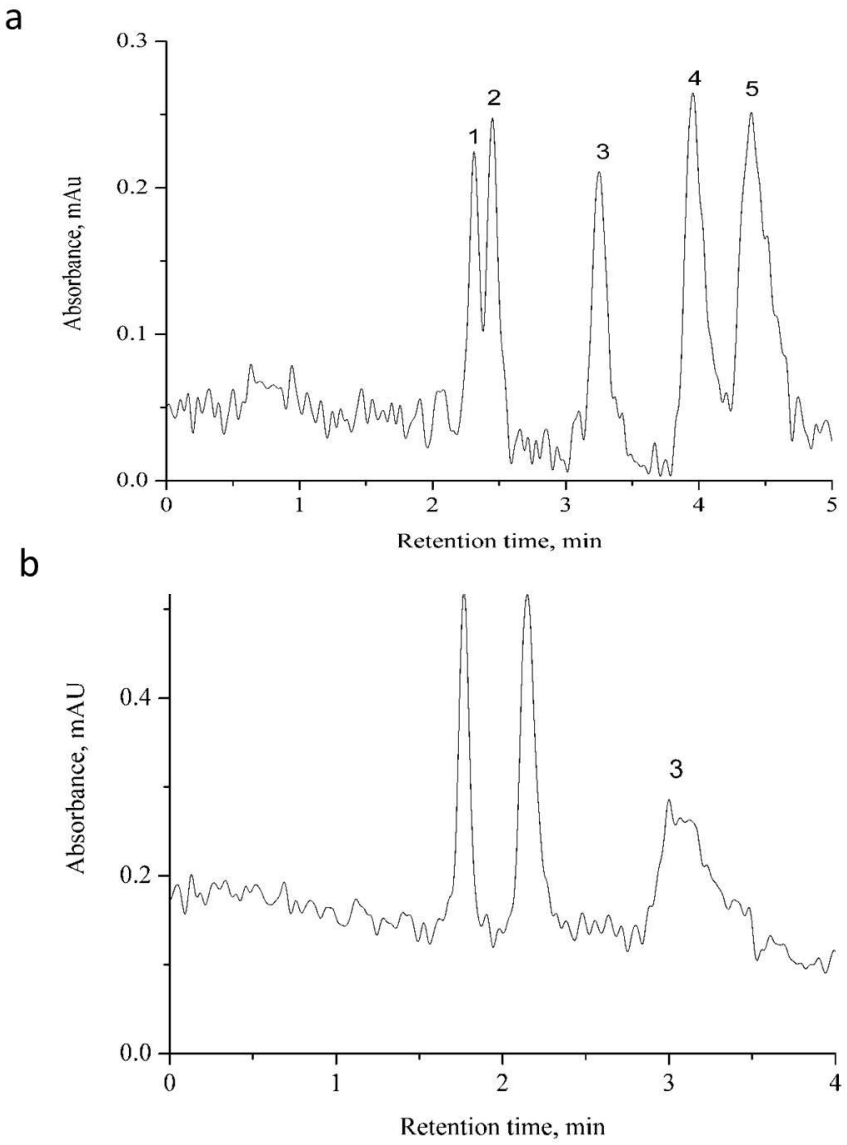

Figure 2.8. HPLC chromatograms for separations of peptides or proteins. A homemade monolithic column was used for HPLC separations, and the HPLC system was driven by 10-unit open-capillary EOPs. The applied voltage to EOPs was 20 kV, and the UV detector was set at 215 nm. The

eluent was 15.9% acetonitrile and 0.1%TFA in DI water. (a) The peptide sample was a mixture of 0.04 mg/mL Gly-Tyr (1), 0.04 mg/mL Val-Tyr-Val (2), 0.04 mg/mL Met enkephalin (3), 0.08 mg/mL Leu enkephalin, and 0.08 mg/mL Angiotension II (5) in 0.1% TFA. (b) The protein sample contained 0.5 mg/mL Ribonuclease A (1), 0.8 mg/mL Insulin (2), and 1.4 mg/mL Cytochrome C.

2.4 Concluding remarks

In this work, we proposed an innovative EOP design which allowed many basic EOP units to be serially stacked to increase the pressure output. With open capillaries to fabricate EOPs, a pressure of ~21.4 MPa was achieved while the maximum flow rate was ~400 nL/min. By simply adding more basic EOP units to the series, the pressure output could be always improved without increasing the applied voltage or decreasing the flow rate. We also demonstrated applications of 10-unit open-capillary EOPs to driving HPLC separations of peptides or proteins. The future work is to develop open-channel EOPs on microchips and to increase both the maximum flow rate and pressure of the constructed EOPs.

The materials in Chapter 2 are adapted from He et al. Journal of Chromatography A 1227 (2012) 253– 258. The copyright was obtained from Wiley (license number: 3365980605472).

Chapter 3: Resolving DNA at Efficiencies of More Than A Million Plates Per Meter Using Bare Narrow Open Capillaries without Sieving Matrices

3.1 Introduction

DNA is a molecule that encodes the hereditary information utilized in humans and all other living organisms. DNA analysis and separation are essential in biological research because they inform us how DNA molecules work and eventually guide us to solve related problems based on DNA examinations.[65-69]

DNA separations are usually performed with slab gel electrophoresis,[70-72] including pulsed-field gel electrophoresis (PFGE).[73,74] As all DNA fragments have similar charge-to-mass ratios, their mobilities depend on their sizes while smaller DNA fragments have greater mobilities. While slab gel electrophoresis is capable of separating DNA fragments nicely and efficiently, its drawbacks, including excessive Joule Heating, tedious operations, and low analysis throughput, have been encouraging increasing interest on developing alternatives for DNA separations.[75-81]

Since being introduced in 1980s by Hjerten,[82] capillary gel electrophoresis (CGE) has shown many advantages over regular gel

electrophoresis. In CGE, separation efficiency was improved, separation time was shortened, and analysis throughput was increased. In 1988, Cohen et al.[33] first reported DNA separations in CGE. With a capillary of 75 μm i.d. as the separation column and 7.5% polyacrylamide gel as the sieving matrix, a DNA mixture, $(dA)_{40-60}$, was baseline separated within 8 minutes. With capillary array gel electrophoresis, analysis throughput of CGE for DNA separation was greatly improved.[83] CGE made significant contributions to Human Genomic Project and currently it is still the workhorse for DNA analysis. However, working with viscous gel in a capillary is never easy. Fabrication of capillaries filled with cross-linked polyacrylamide gel is difficult due to bubble formation. Additionally, preparing cross-linked gel reproducibly is a challenging task. Using linear polyacrylamide gel for DNA separations can address these issues to some extent. The linear gel can be pressurized into the separation capillary for loading and the gel can be replaced after each run. Therefore, the run-to-run reproducibility is improved. However, high pressures are required for loading and replacing the gel. Additionally, preparing linear polyacrylamide gel is tedious and time-consuming. To completely resolve the problems related with gel, DNA separations were proposed to be performed in free solutions.

Free-solution electrophoresis is not capable of separating DNA fragments because all DNA fragments have similar charge-to-mass ratios and, as a result, they all have similar electrophoretic mobilities. In 1992, Noolandi[84] proposed a new concept for DNA separations in free solutions by capillary electrophoresis. By attaching a perturbing entity, which includes proteins, viruses, and charged spheres, to DNA molecules, the charge-to-mass ratios of DNA fragments were changed and consequently varying electrophoretic mobilities were generated. Therefore, DNA fragments were expected to be separated in free solutions. This concept was later named end-labeled free-solution electrophoresis (ELFSE) and its theoretical limits on resolving DNA fragments in free solutions were predicted based on a free-draining coil model.[85] In 1998, Heller et al.[45] experimentally validated this concept and double-strand DNA fragments were electrophoretically separated in free solutions for the first time. After 20+ years of development, ELFSE has become the most successful technique for DNA separations in free solutions.[86-90]

DNA separations were also performed in free solutions based on liquid chromatography (LC). For instance, in 1995, Huber et al.[91] successfully separated DNA fragments ranging from 51 to 2176 bp with ion-pair reverse-phase high-performance liquid chromatography (IP-RP-HPLC). By plotting the capacity factor against logarithm molecular weight,

a good correlation between retention time and DNA length was obtained, indicating that IP-RP-HPLC was capable of separating DNA fragments without using gel. Later, Dickman[92] investigated the effect of structure and sequence on free-solution DNA separations in IP-RP-HPLC, and the results indicated that large non-canonical structures could make DNA separation independent of size while sequence effects may potentially influence retention of double-strand DNA fragments. Other LC modes, such as size-exclusion chromatography[93-95] and slalom chromatography,[96,97] were also adopted for DNA separations in free solutions, and they were proved to be useful tools for DNA research.[98,99]

Beyond ELFSE and HPLC, the techniques for gel-free DNA separations also include anomalous radial migration, [50,100], DNA prism,[48] and entropic trapping.[49,101] While these techniques were capable of separating DNA fragments in free solutions, none of them has the resolving power which is comparable to that of gel electrophoresis. Recently, our group developed a new technique for DNA separations in free solutions. As the technique was performed in a bare narrow capillary and DNA separations were based on hydrodynamic chromatography, it was named Bare Narrow Capillary Hydrodynamic Chromatography (BaNC-HDC).[7,8] In a narrow capillary filled with a free solution, a Poiseuille flow is induced as a pressure is applied and the stream in the center of the capillary moves

faster than that near the wall. When DNA molecules migrate with the Poiseuille flow as particles through the narrow capillary, larger fragments migrate faster because they have larger effective diameter and cannot access the capillary wall as closely as smaller ones do. Therefore, larger fragments are eluted earlier than smaller ones, and this is the basis for DNA separations in BaNC-HDC. With BaNC-HDC, DNA fragments ranging from 75 bp to 106 kbp were separated in a single run[9] and a quadratic model was established to study the transport mechanism of DNA molecules in a narrow capillary.[11] In this work, by investigating the effect of elution pressure and temperature on DNA separations in Ba-NC-HDC, we reported the extremely high efficiency of BaNC-HDC and revealed its unique behaviors in the van Deemter curves. The ultimate goal is to develop a rapid, automatic, and high-efficiency technique for DNA separations and analysis without using any sieving matrix.

3.2 Experimental section

3.2.1 Reagents and chemicals

GeneRuler^{TM} 1-kbp Plus DNA Ladder (SM1331) was purchased from Fermentas Life Sciences Inc. (Glen Burnie, MD), and YOYO-1 was obtained from Molecular Probes (Eugene, OR). Ammonium acetate (NH_4Ac), ammonium hydroxide (NH_4OH), and fluorescein were products

of Fisher Scientific (Fisher, PA). Fused-silica capillaries were supplied by Polymicro Technologies (Phoenix, AZ).

3.2.2 Preparation of separation buffer and standard samples

5 mM NH_4Ac was prepared by diluting 400 mM stock solution with DDI water and pH was adjusted to ~8.0 with concentrated NH_4OH, and it was filtered through 0.22-μm filter (VWR, TX) before use. 1 mM fluorescein stock solution was prepared by dissolving the appropriate amount of fluorescein powder in separation buffer (5 mM NH_4Ac/NH_4OH, pH ~8.0), and working standard solutions were prepared by diluting the fluorescein stock solution with separation buffer at ratios as needed. A sample of 50 ng/μL 1-kbp plus DNA ladder was prepared by mixing 44.5 μL separation buffer, 5 μL 500 ng/μL DNA, and 0.5 μL YOYO-1, and different concentrations of standard DNA solutions were made from this stock solution by diluting with separation buffer at ratios as needed. Sterilized DDI water from a Nanopure^{TM} Infinity Ultrapure Water System (Barnstead, Newton, WA) was used throughout. All solutions were stored at 4 ^{0}C.

3.2.3 Experimental setup

Figure 3.1 presents experimental setup, which consisted of a bare narrow capillary, an LC pump, a chip injector, and a confocal laser induced

fluorescence (LIF) detector. A restriction capillary of 55 cm length and 50 μm i.d. was integrated between the LC pump and the chip injector, and the pressure output of LC pump was controlled to be in the range of 100 – 4000 psi by tuning the flow rate from 0.013 to 0.500 mL/min. The bare capillary was of 2 μm i.d., and it was used as the column for DNA separations in free solutions.

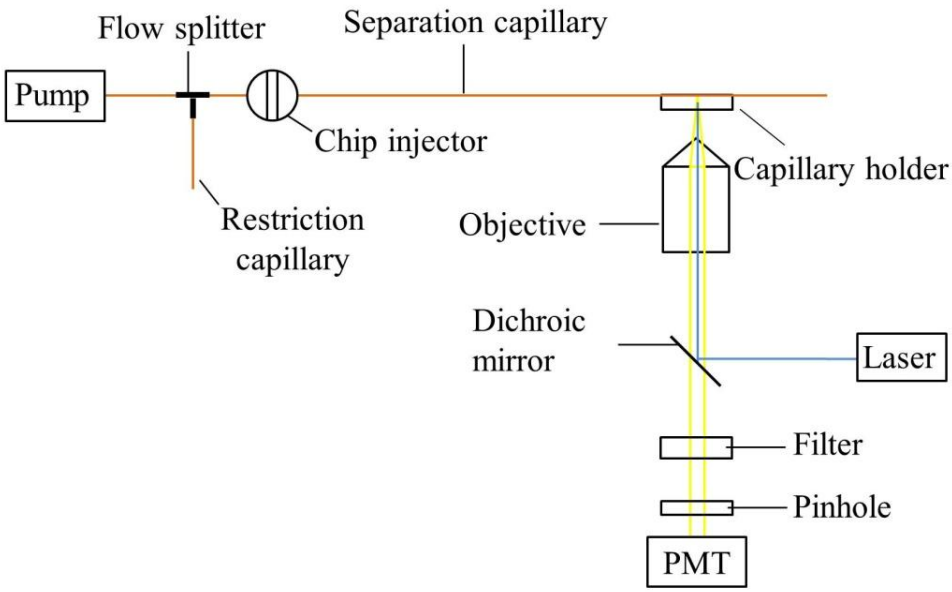

Figure 3.1. Schematic diagram of experimental setup for BaNC-HDC.

The chip injector was in-laboratory fabricated, and it was composed of an on-chip cross and a commercial six-port valve (C5-2006, VICI, Houston, TX). The separation capillary and three auxiliary capillaries were

attached to the on-chip cross with epoxy adhesive. The on-chip cross had round channels of ~380 μm i.d., and the round channels were fabricated with standard photolithographic technologies as reported previously.[102] Briefly, with a photomask, a symmetric pattern which contained sixteen crosses was generated on the photoresist layer spin-coated on wafers. After the Au/Cr layer was etched off, the unveiled glass was etched in concentrated HF solution for ~27 min. The formed grooves were semicircular because the line-width (10 μm) on photomask was much smaller than the diameter (380 μm) of grooves. After two wafers were face-to-face aligned and thermally bonded, round channels were formed. Crosses were produced by dicing the above fabricated chip.

The LIF detector was in-laboratory built, and it was basically a duplicate of the system we previously reported.[7,8] Briefly, a 488-nm beam generated by an argon ion laser (Laserphysics, Salt Lake City, UT, USA) was reflected by a dichroic mirror (Q505LP, Chroma Technology, Rockingham, VT, USA) and then focused onto the window of the separation capillary through an objective lens (206 and 0.5 NA, Rolyn Optics, Covina, CA, USA). Fluorescence emitted from analytes was collimated by the same objective lens, and collected by a photosensor module (H5784-01, Hamamatsu, Japan) after sequently passing through the dichroic mirror, an interference band-pass filter (532 nm), and a 2-mm

pinhole. The output of the photosensor module was acquired with a MCC data acquisition board (USB-FS1608, Measurement Computing Corporation, Norton, MA), and the data was processed with an in-laboratory written Labview program.

3.2.4 Injection scheme

In BaNC-HDC, only picoliters of samples were required for each assay. To realize sample injection at picoliter level, a chip injector was employed. This chip injector was composed of an on-chip cross and a commercial six-port valve. As shown in Figure 3.2a, two ends of the on-chip cross were connected to the six-port valve, and there were two positions on the six-port valve, "Open" (indicated as open dots) and "Block" (indicated as solid dots). The separation capillary and an auxiliary capillary were attached to the other ends of the cross with epoxy adhesive.

The sample solution was first aspirated into the cross section by applying vacuum to waste (W) while keeping the six-port valve in "Open" position and the flow rate of LC pump zero (see Figure 3.2b-*I*). After switching the valve to "Blocked" position, a slight portion of the sample in the cross section was pressurized into the separation capillary by turning on the LC pump to 0.013 mL/min (see Figure 3.2b-*II*). Switching the valve back to the "Open" position, the sample residue in the cross section was

flushed away by turning up LC pump to 0.15 mL/min (see Figure 3.2b-*III*). After flushing, the cross was blocked again and DNA separations were achieved at different pressures by tuning the flow rate of LC pump (see Figure 3.2b-*IV*). This injection scheme was time-control, and the injected sample volume could be accurately controlled by adjusting the injection time while keeping the injection pressure constant. The vacuuming time in step *I* (Figure 3.2b-*I*) and the flushing time in step *III* (Figure 3.2b-*III*) were 1.5 min and 2.0 min, respectively. The injection volume was controlled in the range of 1.2 – 6.5 pL while the separation pressure was adjusted in the range of 100 – 4000 psi by tuning the flow rate of the LC pump in the range of 0.013 – 0.500 mL/min.

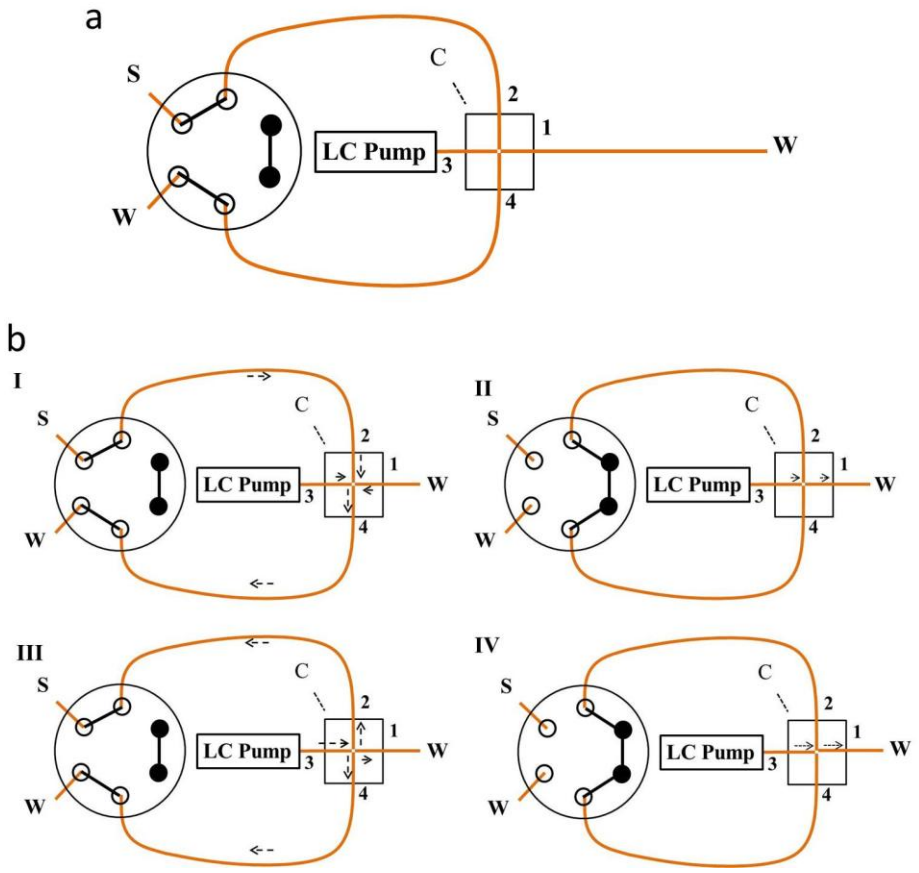

Figure 3.2. Injection schemes in BaNC-HDC. (a) Schematic diagram of a chip injector. (b) Schematic diagram describing the steps for sample injections in BaNC-HDC. A six-port valve was shown on the left. The solid dots indicated that these ports were blocked. Capillaries connected to positions 1, 2, 3, and 4 on the chip injector are separation capillary, sample capillary, pump capillary, and waste capillary, respectively.

3.2.5 Alignment of the detection widow with LIF detector

Referring back to Figure 3.2b, 1 μM fluorescein solution was aspirated into the cross section through the sample capillary by applying vacuum to the waste capillary while keeping the chip injector on "Open" position and the flow rate of LC pump zero. The six-port valve was then switched to "Block" position to block the cross, and the fluorescein solution was pressurized into the separation capillary by turning on LC pump to 0.125 mL/min. While keeping the flow rate of LC pump constant, the fluorescein solution continuously flushed across the detection window (to avoid fluorescein intensity decay caused by photobleaching). The position of the detection window was adjusted via a translation stage while the fluorescence signal was monitored. Once the maximum signal output was reached, the x, y and z positions of the translation stage were locked, and the detection window was aligned with the optical system.

3.3 Results and discussion

When we worked on gel-free DNA separations in BaNC-HDC, it was found that separation resolutions could be improved by simply decreasing elution pressure in the range of 100 – 4000 psi. This phenomenon was assumed to be due to the extremely small diffusion coefficients of DNA fragments in the confined environment (a 2 μm i.d. capillary). To prove this

hypothesis, the behaviors of DNA fragments in the separation capillary were investigated.

3.3.1 Effect of eluent velocity on DNA separations

To investigate the effect of eluent velocity on DNA separations in BaNC-HDC, elution pressure was decreased from 2000 psi to 100 psi. Figure 3.3 presents the chromatograms at five different elution pressures (100, 200, 400, 1000, and 2000 psi). As expected, separation time was shortened by increasing elution pressure and, on the other hand, resolutions were decreased as elution pressure was increased from 100 to 2000 psi (see Figure 3.4).

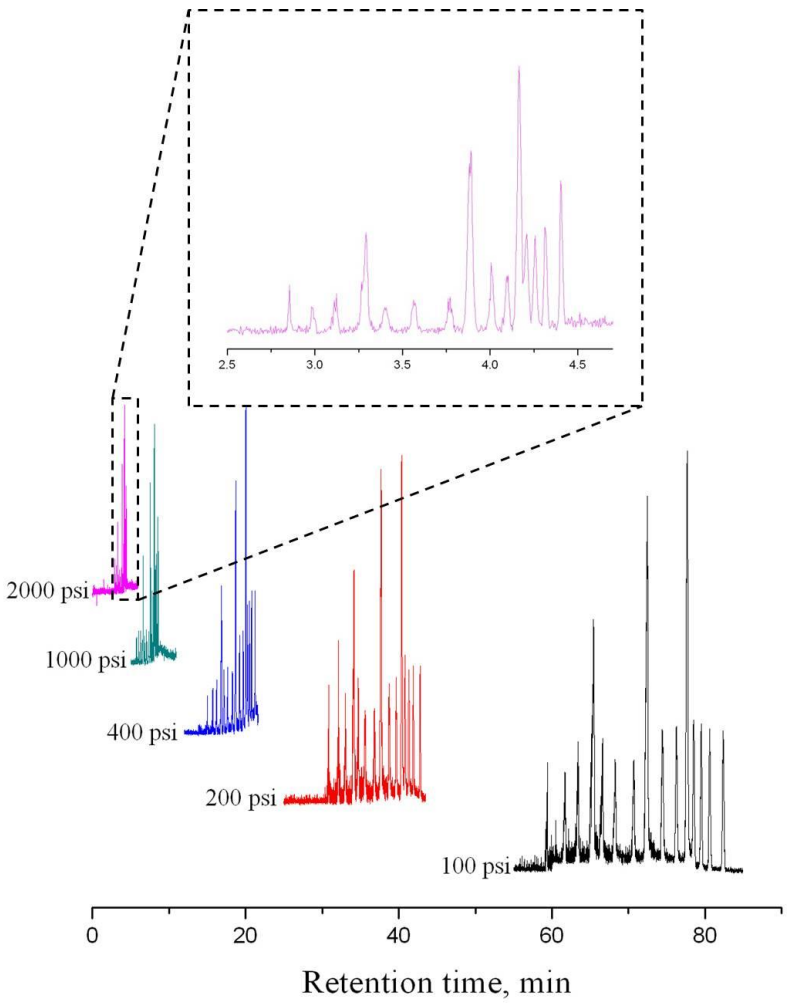

Figure 3.3. Typical chromatograms obtained at different elution pressures. Eluent, 5 mM NH_4Ac/NH_4OH at pH ~8.0. The sample was 20 ng/μL GeneRuler^{TM} 1-kbp Plus DNA Ladder, which contained 15 DNA fragments. The DNA concentrations were 0.8 ng/μL for 2, 3, 4, 7, 10 and 20 kbp fragments, 1 ng/μL for 0.075, 0.2, 0.3, 0.4, 0.7, and 1 kbp framents, 3.0 ng/μL for 0.5 and 5 kbp fragments, and 3.2 ng/μL for the 1.5 kbp fragments,

respectively. The separation capillary was of 2 μm i.d. and 70 cm total length (65 cm effective). The injection volume was estimated to be ~2.4 pL.

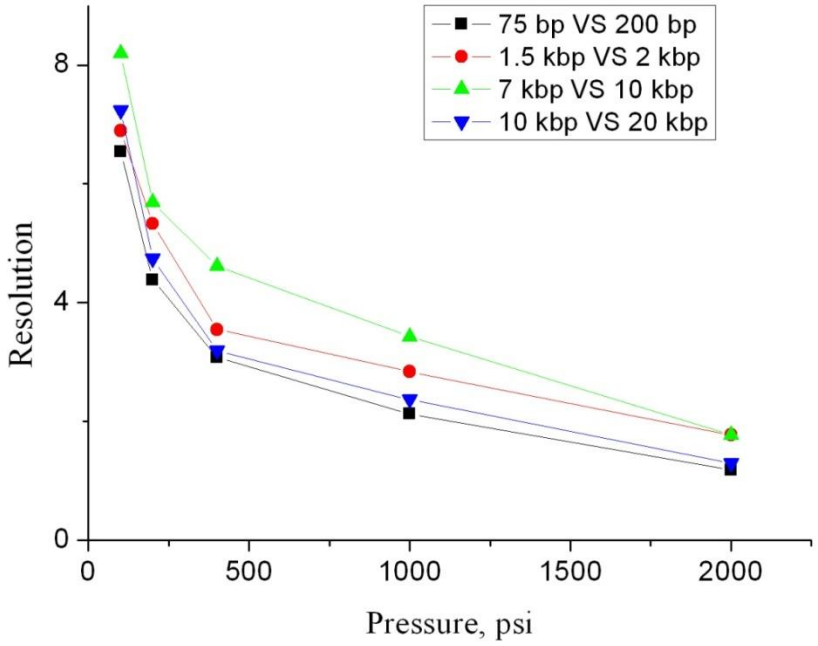

Figure 3.4. Effect of elution pressure on resolutions. All data were obtained based on Figure 3.3.

The effect of elution pressure on efficiencies was also investigated. As shown in Figure 3.5a, while increasing elution pressure shortened analysis time, efficiencies became worse as elution pressure increased. At 100 psi, efficiencies of more than $4*10^5$ theoretical plate per meter were

achieved for all 15 DNA fragments in GeneRuler^{TM} 1-kbp Plus Ladder, and 4 fragments (75, 200, 300, and 400 bp) had efficiencies of more than 1 million theoretical plates per meter. As elution pressure was increased to 2000 psi, efficiencies decreased while analysis time was shortened to less than 5 minutes. However, 10 DNA fragments (0.7, 1, 1.5, 2, 3, 4, 5, 7, 10, and 20 kbp) still had efficiencies of more than $1*10^5$ theoretical plates per meter. These exceptionally high efficiencies were first reported in a chromatographic format in this work.

The relationship between the height equivalent to a theoretical plate (HETP) and eluent velocity was also plotted. As shown in Figure 3.5b, HETP increased as eluent velocity increased in the whole range. Actually, a set of straight lines were obtained, and linear correlation coefficients were in the range of 0.900 – 0.993.

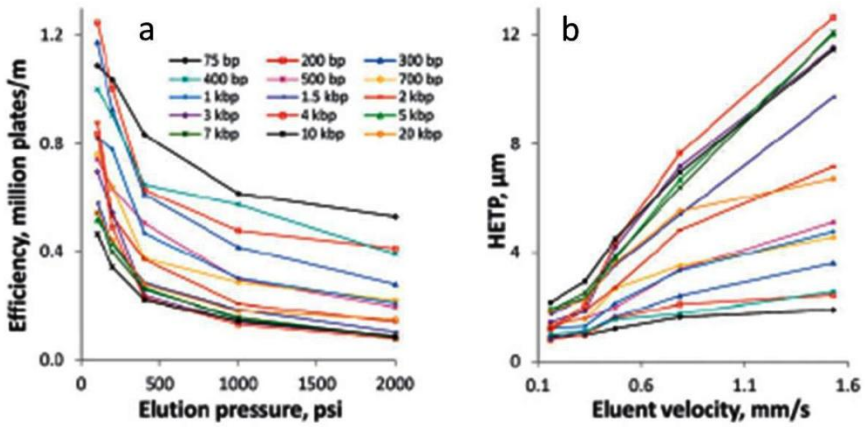

Figure 3.5. Effect of elution pressure on DNA separations in BaNC-HDC. (a) Relationship between efficiencies and elution pressure. (C) Relationship between HETP and eluent velocity. All data were obtained based on Figure 3.3.

According to the chromatographic band-evolving theory, simplified van Deemter equation relates HETP to eluent velocity (u) as follows,

$$HETP = A + \frac{B}{u} + C * u \qquad (3.1)$$

where A, B, and C are constants; A is Eddy-diffusion parameter, coming from non-ideal packing; B term relates to diffusion of the eluting particles in the longitudinal direction; C term is caused by the resistance to analyte mass transfer between the mobile phase and the stationary phase. The

straight lines in Figure 3.3C indicated that the band-broadening effecting caused by *B* term could be neglected (*B*=0), which may be due to the reduced diffusion coefficients of DNA fragments in the confined environment (a 2 μm i.d. capillary). It has been reported that molecular diffusion in nanopores can be reduced by orders of magnitude.[103]

To confirm the above-mentioned observation, a dye (fluorescein), which has low molecular weight, was mixed with four DNA fragments (0.075, 1.5, 5, and 20 kbp), and the mixture was separated with BaNC-HDC. Elution pressure was adjusted in the range of 100 – 4000 psi by tuning the flow rate of LC pump in the range of 0.013 – 0.500 mL/min (see Figure 3.6). By plotting HETP of fluorescein *versus* eluent velocity, a regular van Deemter curve was obtained (see Figure 3.7a). As the separation capillary was narrow (2 μm i.d.) and the diffusion coefficient of fluorescein was relatively large, fluorescein molecules were able to rapidly migrate from the center to the wall of the separation capillary and, as a result, the *C* term for fluorescein was small. When HETP of DNA fragments was plotted against eluent velocity, HETP did not increase as eluent velocity decreased even at extremely low velocity (see Figure 3.7b). As mentioned above, this should be due to the small diffusion coefficients of DNA fragments in the narrow capillary. As the confined environment significantly reduced the diffusion coefficients of DNA fragments, the band-broadening caused by diffusion

could be neglected and, as a result, *B* term in van Deemter equation disappeared. Additionally, as the separation capillary used in this work was unpacked, Eddy-diffusion parameter (*A* term in van Deemter equation) was expected to be zero. However, as shown in Figure 3.7b, the obtained *A* values were in the range of 1 – 5 μm. This was likely due to the finite lengths of the initial sample plugs.

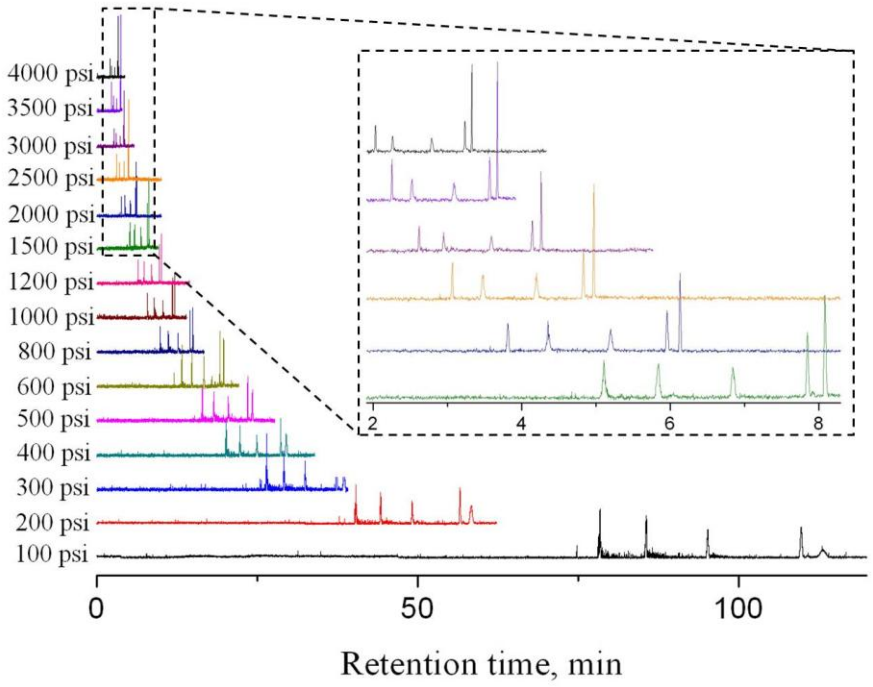

Figure 3.6. Chromatograms obtained at different elution pressures. The sample was a mixture of fluorescein and 4 DNA fragments (0.075, 1.5, 5, and 20 kbp). Each DNA fragment was at a concentration of 2 ng/μL while

the concentration of fluorescein was 200 nM. The separation capillary was of 2 μm i.d. and 80 cm total length (75 cm effective). All other conditions were as in Figure 3.3.

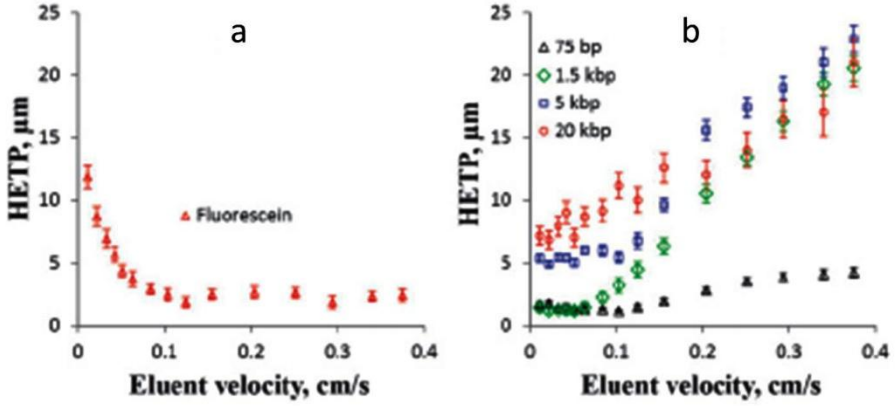

Figure 3.7 Effect of eluent velocity on separation efficiencies. (a) Relationship between fluorescein HETP and eluent velocity. (b) Relationship between DNA HETP and eluent velocity. All data were obtained based on Figure 3.6.

3.3.2 Effect of temperature on DNA separations

As previously reported,[104] separation time in BaNC-HDC could also be shortened by increasing separation temperature. In this work, the effect of temperature on DNA separations in BaNC-HDC was investigated in the

range of 25 – 80^{0}C. Separation temperature was controlled by submerging the separation capillary in a water bath.

Figure 3.8a presents typical chromatograms of DNA separations in BaNC-HDC at different temperatures. Separation time was almost halved as temperature was increased from 25^{0}C to 80^{0}C. On the other hand, efficiencies decreased as temperature was increased (see Figure 3.8b), which should be due to the increased eluent velocity at increased temperature.

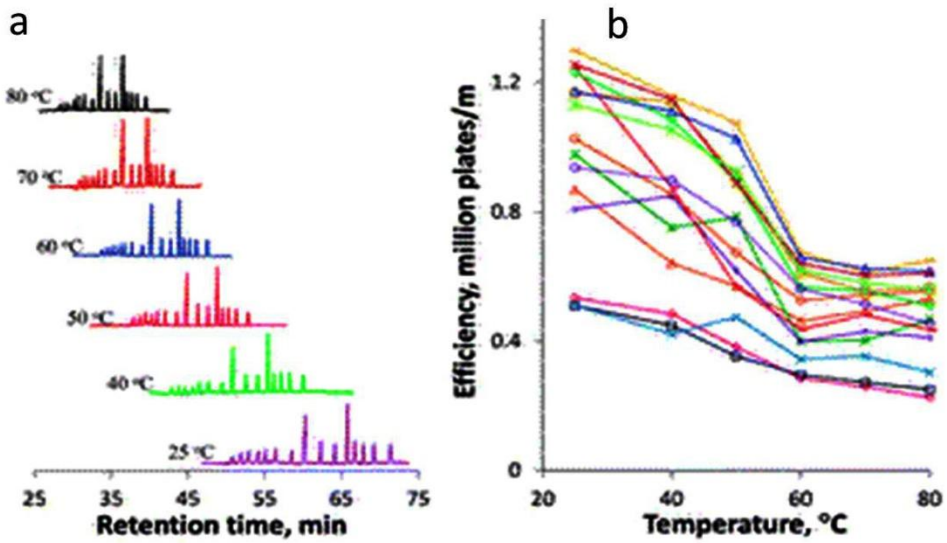

Figure 3.8. Effect of temperature on DNA separations in BaNC-HDC. (a) Typical chromatograms of DNA separations in BaNC-HDC at different temperatures. The DNA mixture had a total concentration of 50 ng/μL. The separation capillary was of 1.5 μm i.d. and 70 cm total length (65 cm

effective). All other conditions were as in Figure 3.3. (b) Effect of temperature on sefficiencies. All data was obtained based on Figure 3.8a.

In a capillary filled with a solution, a laminar flow is induced as a pressure is applied. According to Hagen-Poiseuille Law, the flow rate through the capillary can be expressed as follows,

$$Q = \Delta P * \frac{\pi d^4}{128 \mu L} \qquad (3.2)$$

where d and L are the inner diameter and length of the capillary; μ is the viscosity of the solution filled in the capillary; Q is the flow rate through the capillary and ΔP is the pressure drop across the capillary. As the liquid viscosity tends to decrease as its temperature increases, the flow rate through the capillary is consequently increased by increasing temperature. Therefore, in this work, separation time was shortened as temperature was increased from 25^0C to 80^0C. Figure 3.9a presents the effect of temperature on eluent velocity in the separation capillary. As expected, the measured eluent velocity increased accordingly as temperature increased. The relationship between relative mobility (the ratio of DNA mobility to eluent mobility) and temperature was also investigated. As shown in Figure 3.9b, for all DNA fragments, relative mobility was not changed as temperature

was increased from 25^0C to 80^0C. This indicated that DNA properties and separation mechanism in BaNC-HDC were not changed in the investigated temperature range.

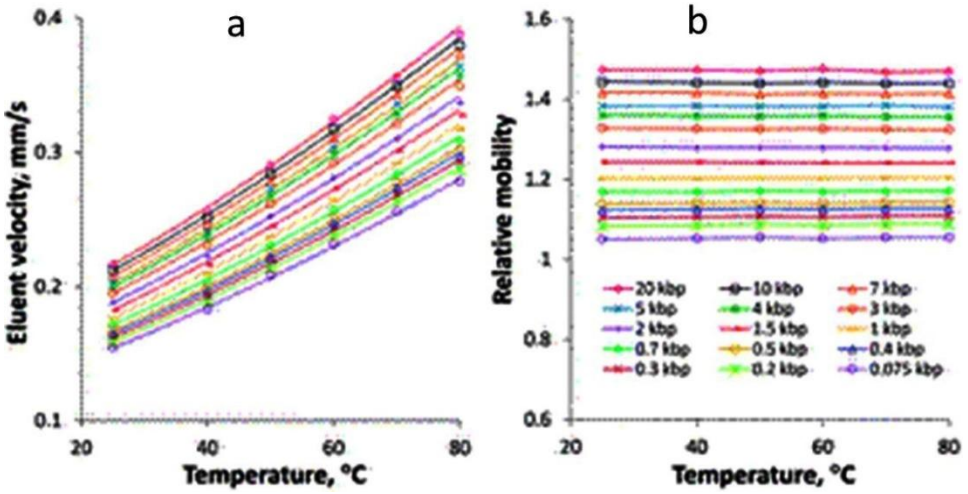

Figure 3.9. Effect of temperature on eluent velocity and relative mobility in BaNC-HDC. (a) Relationship between temperature and eluent velocity. (b) Relationship between temperature and relative mobility (the ratio of DNA velocity to eluent velocity). All data were obtained based on Figure 3.8a.

3.4 Concluding remarks

In this work, we demonstrated the power of BaNC-HDC to separate DNA fragments without using any sieving matrix. With BaNC-HDC, efficiencies of more than one million theoretical plates per meter could be

readily achieved. This was believed to be due to the extremely small diffusion coefficients of DNA fragments in the narrow separation capillary (2 μm i.d.). The confined environment significantly reduced the diffusion coefficients of DNA fragments and, as a result, the band-broadening caused by diffusion could be neglected. Separation time could always be shortened by increasing elution pressure, but the time saving was accompanied with the loss of efficiencies. Future work will be devoted to integrating the BaNC-HDC system and automating all involved operations. BaNC-HDC is expected to become an excellent alternative to slab gel electrophoresis for rapid and automatic DNA analysis.

The materials in Chapter 3 are adapted from Zhu et al. Chemical Communication, 49 (2013) 2897-2899. Reproduced by permission of The Royal Society of Chemistry.

Chapter 4: Integrated Bare-Narrow-Capillary Hydrodynamic-Chromatography for Gel-Free DNA Separations

4.1 Introduction

DNA analysis is crucial in the field of molecular biology, and DNA separations are typically required in DNA analysis for identification, purification, or fractionation. Traditionally, DNA separations are carried out with agarose gel electrophoresis[105], including pulsed field gel electrophoresis[29]. To improve resolution, reduce analysis time, and increase throughput, a shift to capillary gel electrophoresis (CGE) or capillary array electrophoresis (CAE) was attempted and excellent separations were achieved[106-108]. However, both CGE and CAE still require viscous gel solutions, which can be difficult to work with, especially when narrow channels are employed. One promising solution to this problem is to separate DNA fragments in free solutions. Unfortunately, DNA cannot normally be separated with free-solution electrophoresis because all DNA molecules have similar mass-to-charge ratios (*m/z*) and, as a result, they have similar electrophoretic mobilities. In 1992, Noolandi[84] proposed a new concept to solve this problem by attaching a charged label molecule to each strand of DNA, generating varying *m/z* values for DNA molecules to be separated. Taking the advantage of this concept, Mayer et al.[85] studied the

theoretical limits of free-solution electrophoresis for DNA separations, and then derived the separation power of the proposed approach and compared it with that of gel electrophoresis. The proposed approach, named end-labeled free-solution electrophoresis (ELFSE), was experimentally validated in the late 1990s[45,49] and already developed into the most successful approach for separating small DNA fragments in free solutions[88-90].

In 2002, Zheng et al.[50] reported a novel mechanism, called redial migration, for separations of large DNA fragments in free solutions based on Poiseuille flow. Due to the Poiseuille flow generated inside a capillary filled with a free solution, DNA molecules deviated away from their electric-field lines. The magnitude of such deviation was size dependent, and consequently DNA fragments were size-dependently separated in free solutions. With this developed mechanism, two model DNA molecules, λDNA and φX174 RF DNA, were baseline separated[100]. Other gel-free approaches for DNA separations include liquid chromatography[92,109], entropic trapping[49], and DNA prism[48]. These approaches, to some extent, overcome the problems brought by gel electrophoresis, and they offer a promising alternative for fast and cost-effective DNA separations.

Recently, our group developed a new technique[7,8,11,51,110,111] for free-solution DNA separations. This technique was performed in a bare narrow

capillary and it was based on hydrodynamic chromatography, the new technique was named Bare Narrow Capillary Hydrodynamic Chromatography (BaNC-HDC). In a narrow capillary filled with a free solution, Poisseuille flow is induced under the influence of pressure differential. The streamlines in the center of the capillary are the fastest while the streamlines near the wall are the slowest. As DNA fragments travel through the capillary, larger DNA fragments cannot access the capillary wall as closely as smaller ones do. Therefore, larger DNA fragments migrate faster through the capillary and they elute earlier in BaNC-HDC than smaller ones. BaNC-HDC was capable of separating DNA fragments from 75 to 106,100 bp in a single run[110], and it also enabled us to separate crude PCR products without further purification[8]. Fast analysis (30 – 160 minutes in total), minimal sample requirement (1-5 pL), and low operation cost make BaNC-HDC an excellent alternative technique to gel electrophoresis for DNA separations.

In all our previous works, BaNC-HDC was driven by regulated gas pressure, which was bulky and required experienced operators to obtain good reproducibility. More importantly, the pressure chamber could only sustain a pressure of ~3.5 MPa, which was not adequate to drive BaNC-HDC for fast DNA separations. In this work, we aimed to use electroosmotic pumps (EOPs) we previously developed to drive BaNC-

HDC for DNA separations. We also developed a microchip injector for sample injections in BaNC-HDC at picoliter level. The constructed 3-unit open-capillary EOPs could provide a pressure of up to 21.4 MPa, allowing the separation of 1-kbp plus DNA ladder to be achieved within 5 minutes. Additionally, with an on-chip cross and an off-chip six-port valve, the developed microchip injector was handily operated and the injected sample volume was accurately controlled at picoliter level. In this work, incorporation of EOPs and a microchip injector into the BaNC-HDC system paved the way to fast and automatic DNA separations in free solutions with "lab-on-chip" technologies.

4.2 Experimental section

4.2.1 Reagents and chemicals

GeneRuler^{TM} 1-kbp Plus DNA ladder (SM1331) was obtained from Fermentas Life Sciences Inc. (Glen Burnie, MD). YOYO-1 was purchased from Molecular Probes (Eugene, OR). Fluorescein, tris(hydroxymethyl) aminomethane (Tris), ethylenediaminetetraacetic acid (EDTA), sodium hydroxide, ammonium acetate, and concentrated hydrochloric acid and ammonium hydroxide were products of Fisher Scientific (Fisher, PA).

10 mM TE buffer was composed of 10 mM Tris/HCl and 1 mM Na_2EDTA at pH 8.0. NH_4OH/NH_4Ac buffer was prepared from 400 mM

NH_4Ac and 100 mM NH_4OH stock solutions. Ultrapure water purified by a Nanopure^{TM} Infinity Ultrapure Water System (Barnstead, Newton, WA) was used for preparing solutions, and all solutions were filtered through 0.22-μm filter (VWR, TX) before being used.

4.2.2 Microchip injector

The developed microchip injector was composed of an on-chip cross and an off-chip six-port valve (see Figure 4.1a). The on-chip cross had round channels of ~170 μm i.d., and the round channels were fabricated as described previously[112]. Briefly, a glass wafer, which was beforehand sputtered with 30 nm Cr and 500 nm Au, was annealed at 150^0C for 1.5 h. After being coated with photoresist, the glass wafer was soft-baked at 85^0C for 20 min. Then, the photoresist was exposed to UV light under the photomask, and the exposed photoresist was developed in MF^{TM}-319 (Rohm and Haas Electronic Materials LLC, Marlborough, MA). After the unveiled Cr/Au was etched off, the wafer was etched in concentrated hydrofluoric acid for ~13 min. After the Cr/Au layer was thoroughly removed, the generated grooves were roughly semicircular because the line-width on the photomask was narrow (5 μm). Round channels were formed by face-to-face aligning and bonding two etched wafers.

As shown in Figure 4.1b, a capillary column (2 μm i.d., 150 μm o.d., and 70 cm length) was glued into a channel with epoxy adhesive, and three other capillaries (20 μm i.d., 150 μm o.d., and 15 cm long) were glued into the other three channels to serve as pump capillary, sample capillary, and waste capillary, respectively. To avoid polyimide scraps shedding from capillary tips into the cross section, polyacrylamide coating on capillary tips was burnt up with mini torch (BernzOmatic®). The zoom-in view of the crossing section of the on-chip injector was shown in Figure 4.1c. The free ends of sample capillary and waste capillary were connected to a six-port valve. The six-port valve can readily block or open the on-chip cross as described in Injection Schemes (Section 4.2.6).

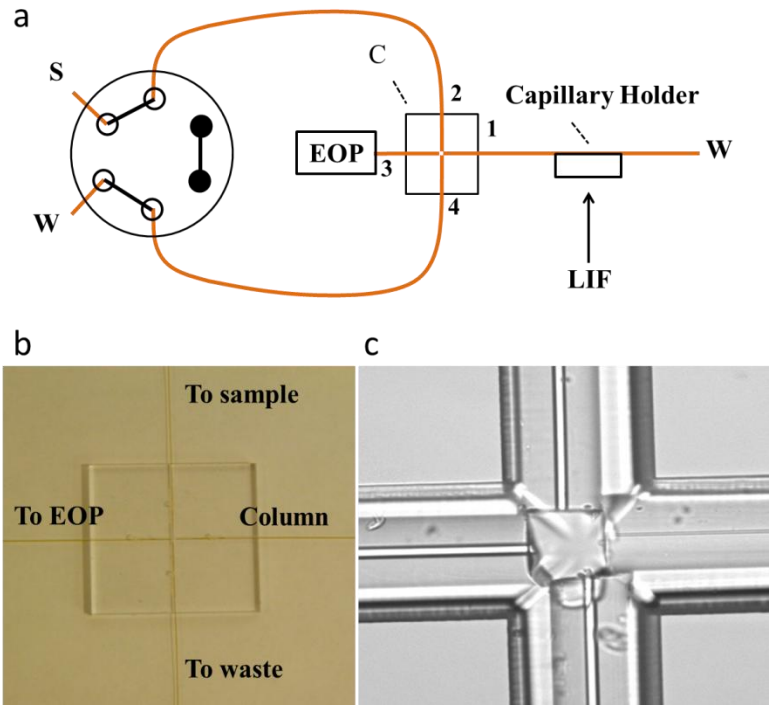

Figure 4.1. Microfabricated injector. (a) Schematic of the on-chip injector. C, on-chip cross; 1, separation capillaries (2 μm i.d., 150 μm o.d., and 70 cm length); 2 – 4, sample capillary, pump capillary, and waste capillary, respectively (all 20 μm i.d., 150 μm o.d., and 15 cm length). (b) Image of the on-chip cross. (c) Zoom-in view of the crossing section in the on-chip injector.

4.2.3 Electroosmotic pumps

Electroosmotic pumps were constructed as previously described[18,113]. Briefly, a basic EOP unit was composed of a +EOP and a –EOP. The +EOP was fabricated with positively coated 5 μm i.d. capillaries while the –EOP was fabricated with bare 2 μm i.d. capillaries, which had negatively charged wall in the pump buffer. 35 pump capillaries were first bundled inside a PEEK tubing, and epoxy adhesive was subsequently applied to the gap between pump capillaries and the PEEK tubing to avoid liquid leakage. +EOP and –EOP were fluidic-ly assembled with a micro Tee. The third lead of the micro Tee was electrically connected to a gel-based bubbleless electrode, which was prepared as previously reported[16]. The free end of the bubbleless electrode was inserted in a bulk buffer solution, where a high voltage was applied through a metal electrode and the electric potential was

extended to the buffer solution in the micro Tee. Since both the inlet and the outlet the EOP unit were grounded, EOP units could be conveniently stacked in series to boost the pumping pressure.

In this work, to obtain fast DNA separations with BaNC-HDC, three EOP units were stacked to increase the pumping pressure as demonstrated in Figure 4.2. As the external voltage increased in the range of 5 – 25 kV, the pumping pressure of the constructed EOP increased linearly (r^2=0.996). The good linear coefficient ensured us to accurately control the pressure needed by adjusting the applied voltage. When 20-kV external voltage was applied, the maximum flow rate of 65.9 nL/min and the maximum pressure of 21.4 MPa were obtained.

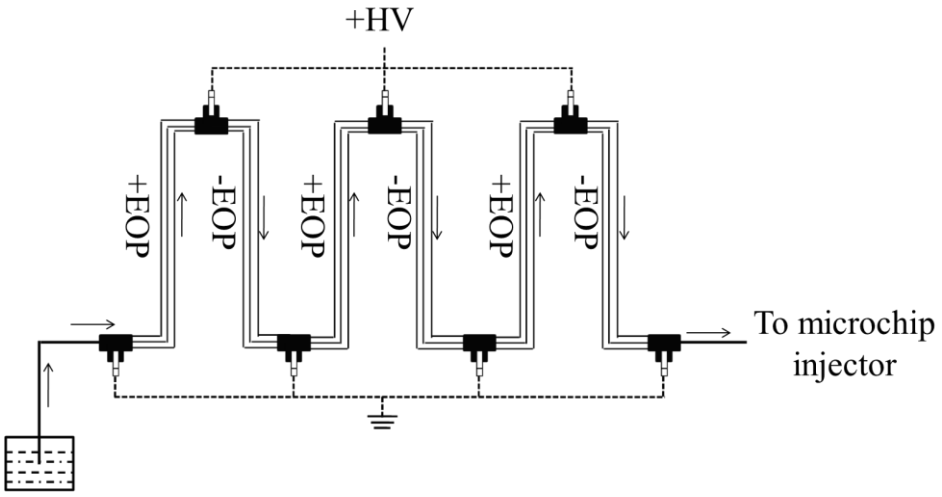

Figure 4.2 Schematic diagram of 3-unit open-capillary EOPs.

4.2.4 Apparatus

As mentioned above, the experimental setup was composed of a 3-unit EOP, a microchip injector, and a bare narrow capillary. The photograph of the apparatus was shown in Figure 4.3, and a quarter was used to demonstrate the relative size of the integrated BaNC-HDC system.

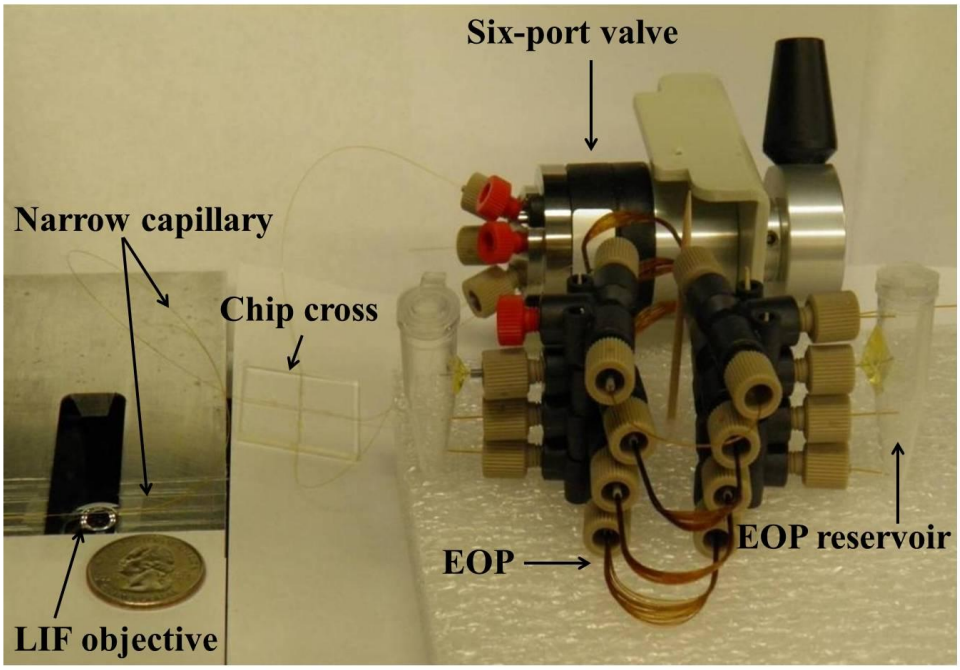

Figure 4.3. Photograph of the apparatus used for BaNC-HDC.

A LIF detector was utilized to monitor the separated DNA fragments. The 3-unit EOP was connected to the free end of the pump capillary to drive DNA separations in BaNC-HDC. The free ends of the sample

capillary and the waste capillary were connected to a six-port valve as discussed above. At an appropriate location (~5 cm from the free end) of the separation capillary, polyimide coating was removed to form the detection window. The detection end of the capillary was affixed to a capillary holder which was attached to an x–y–z translation stage to align the detection window with the optical system to maximize the fluorescent output.

The utilized LIF detector was basically a duplicate of the system we reported previously[7,8]. Briefly, a 488-nm beam from an argon ion laser (Laserphysics, Salt Lake City, UT, USA) was reflected by a dichroic mirror (Q505LP, Chroma Technology, Rockingham, VT, USA) and focused onto the narrow capillary through an objective lens (206 and 0.5 NA, Rolyn Optics, Covina, CA, USA). Fluorescence from the narrow capillary was collimated by the same objective lens, and collected by a photosensor module (H5784-01, Hamamatsu, Japan) after passing through the dichroic mirror, an interference band-pass filter (532 nm), and a 2-mm pinhole. The output of the photosensor module was acquired with a MCC data acquisition board (USB-FS1608, Measurement Computing Corporation, Norton, MA) The data were acquired and treated with program written in-laboratory with Labview (National Instruments, Austin, TX).

4.2.5 Alignment of the detection window with LIF detector

Referring back to Figure 4.1, 1 μM fluorescein solution was aspirated into the cross section from the sample capillary by applying vacuum to the waste capillary while keeping the six-port valve "Open" and EOPs powered off. After switching the valve to "Block" position, the fluorescein solution was driven into the separation column by EOPs. By keeping the EOP voltage constant, the fluorescein solution flushed across the detection window (to avoid fluorescein intensity decay caused by photobleaching). The position of the detection window was adjusted via the translation stage while the fluorescence signal was monitored. Once the maximum signal output was reached, the x, y and z positions of the translation stage were locked and the detection window was aligned with the optical system.

4.2.6 Injection schemes

In this work, we developed a microchip injector, which was composed of an on-chip cross and an off-chip six-port valve. As shown in Figure 4.4a, the sample was aspirated into the cross section by applying vacuum to the waste capillary (W) while keeping the valve in "Open" position and EOPs powered off. After switching the valve to the "Blocked" position (the solid dots indicate these ports were blocked), a portion of the sample in the cross section was injected into the separation column by

EOPs (see Figure 4.4b). Switching the valve back to the "Open" position, the sample residue in the cross section was flushed away with EOPs (see Figure 4.4c). After flushing, the valve was blocked again and DNA separations were performed by keeping EOPs powered on (see Figure 4.4d). This injection was time-control, and the injected sample volume could be accurately controlled by adjusting the injection time while keeping the injection pressure constant. The vacuuming time in step *a* (Figure 4.4a) and the flushing time in step *c* (Figure 4.4c) were 1.5 and 2.0 minutes, respectively. The injection volume was controlled in the range of 1.2 – 6.5 pL, and the elution pressure was controlled in the range of 0.69 – 14 MPa by tuning the applied voltage to 3-unit EOPs in the range of 550 V – 11.1 kV.

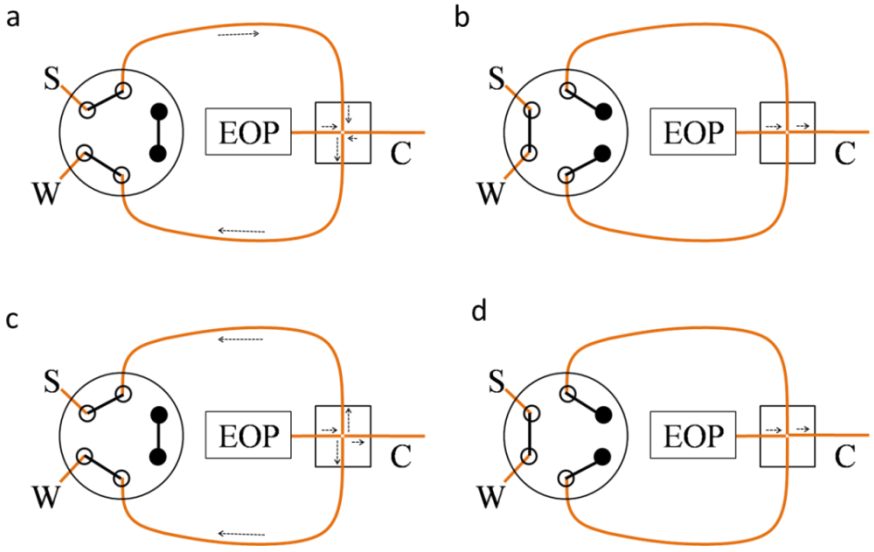

Figure 4.4. Schematic diagrams describing the injection procedures.

4.3 Results and discussion

In all our previous works, BaNC-HDC was driven by regulated gas pressure, which was bulky and required experienced operators to obtain good reproducibility. In addition, the pressure provided by regulated gas was not adequate for fast DNA separations in BaNC-HDC if the separation capillary is long. In this work, to achieve fast and automatic DNA separations, we incorporated a 3-unit EOP and a microchip injector into the BaNC-HDC system. However, as the applied pressure increased, resolutions became worse while the analysis time was shortened. To obtain 5-minute baseline separation, separation conditions, including column length, buffer concentration and composition, and injected sample volume, were optimized based on the results reported previously.

4.3.1 Effect of the buffer composition and concentration on DNA separations

In this work, TE buffer was first employed as the separation buffer. In the concentration range of 1 – 200 mM, TE buffer gave comparable resolutions while the retention time increased gradually as the concentration increased. The peak areas fluctuated when the buffer concentration was below 10 mM and all peaks disappeared when the buffer concentration was

decreased to 0.2 mM. Therefore, 10 mM TE was used for the following experiments.

To simplify the BaNC-HDC system, the EOP solution, 5 mM NH_4Ac at pH ~6.8, was examined to be used as the separation buffer. Initially, no peaks were observed. Considering that pH could shift the excitation wavelength of labeled DNA fragment and, as a result, significantly reduced fluorescence signals, the effect of the buffer pH on sensitivity of the BaNC-HDC system was investigated. Signals recovered as the buffer pH was increased to ~8.0. In an attempt to shorten the analysis time, the buffer concentration was decreased from 5 mM to 0.2 mM while keeping pH at ~8.0. As the buffer concentration decreased, the retention time decreased but the decrease was not significant (see Figure 4.5). Considering that too low buffer capacity may cause the EOP unstable, 5 mM NH_4Ac was selected as both the separation buffer and the EOP solution in the following experiments.

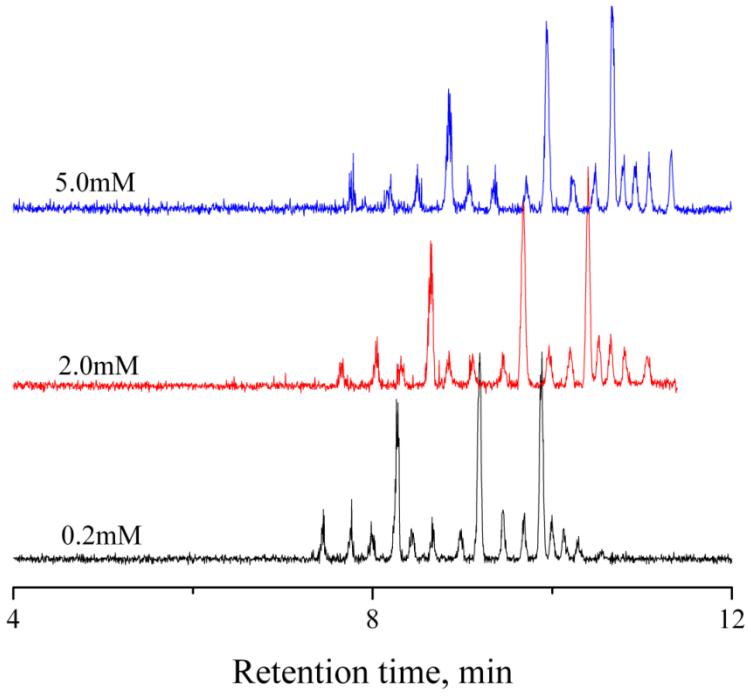

Figure 4.5. Effect of the buffer concentration on DNA separations in BaNC-HDC. The separation capillary had a total length of 47.5 cm (42.5 cm effective). The eluent was NH_4Ac/NH_4OH (pH=8.0) and the concentration was as shown in the figure. The estimated injection volume was 2.4 pL and the elution pressure was 2.1 MPa. The sample contained 15 DNA fragments, and the total DNA concentration was 20 ng/μL; 3.2 ng/μL for the 1.5 kbp fragment, 3 ng/μL for the 0.5, and 5 kbp fragments, 1 ng/μL for the 0.075, 0.2, 0.3, 0.4, 0.7, and 1 kbp fragments, and 0.8 ng/μL for the 2, 3, 4, 7, 10, and 20 kbp fragments, respectively.

4.3.2 Effect of injected sample volume on DNA separations

In chromatography separations, the injected sample volume is critical because it determines the width of the initial sample zone and, as a result, affects the width of the final zone evolved by diffusion or diffusion-like processes. To keep the final band width at a minimum, the effect of the injected sample volume on separations was investigated from 6.5 pL to 1.2 pL. As shown in Figure 4.6, resolutions improved as the injected sample volume decreased. However, when the injected sample volume was below 2.4 pL, further decreasing the injection volume significantly decreased concentration sensitivity in BaNC-HDC while resolutions were not considerably improved. Additionally, when the injection volume was too small, the injection time was too short to be precisely controlled and reproducibility for peak widths became poor. Therefore, 2.4 pL was selected as the injected sample volume in the following investigations.

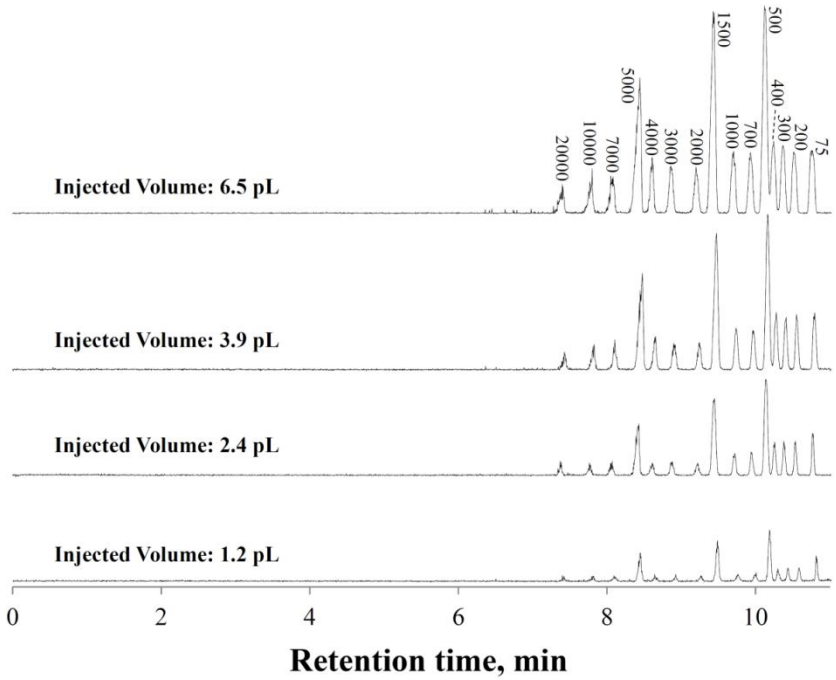

Figure 4.6. Effect of the injection volume on DNA separations in BaNC-HDC. The eluent was 5 mM NH_4Ac/NH_4OH (pH=8.0), and the estimated injection volume was as shown in the figure. Other conditions were the same as in Figure 4.5.

4.3.3 Effect of column length on DNA separations

In BaNC – HDC, column length is another critical factor to consider because it may affect both resolution and efficiency. In this work, two column lengths, 45 cm and 70 cm, were first examined. Compared with the 45-cm column, the 70-cm column gave improved resolutions and decreased

height equivalent to a theoretical plate. However, in BaNC-HDC, to keep the separation time constant, the required pressure will increase exponentially as the column length increases. In this work, to control the elution pressure in a reasonable range, the column length was not examined above 70 cm.

While the total column length was fixed at ~70 cm, different effective column lengths were examined to investigate its effect on DNA separations in BaNC-HDC. Generally, multiple widows were generated with a sharp blade at different distances from the inlet of the separation capillary. As shown in Figure 4.7, all 15 DNA fragments eluted out within 2.3 min when the effective column length was 14.7 cm. However, some DNA fragments were not baseline separated. Increasing the effective column length significantly improved the resolutions, but the required time increased proportionally. Therefore, the effective column length could be adjusted depending on the analysis requirements.

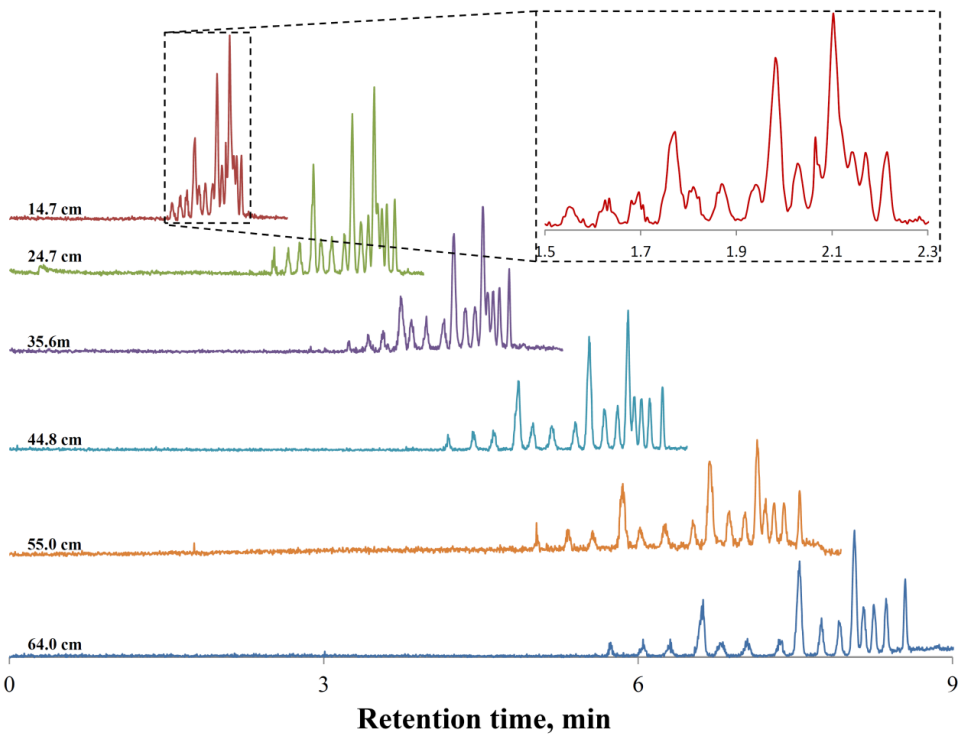

Fig. 4.7 Effect of the effective column length on DNA separations in BaNC-HDC. The total capillary length was 69.4 cm, and different effective lengths were obtained by generating windows at different positions of the separation capillary. The elution pressure was 6.9 MPa. The inset exhibits an expanded view of the fastest separation. All other conditions were as in Figure 4.5.

4.3.4 Effect of the elution pressure on DNA separations

In an attempt to shorten the analysis time, the elution pressure was increased from 0.69 to 14 MPa. As expected, the retention time was inversely proportional to the elution pressure (see Figure 4.8). However, resolutions became worse as the elution pressure increased, and Figure 4.9 demonstrated the change of resolutions between 400-bp and 500-bp DNA fragments as the elution pressure was changed. The driving pressure was controlled by adjusting the applied voltage, and the linear relationship between the maximum pressure and the applied voltage for the constructed 3-unit EOP was excellent (R^2=0.994). When 13.8-MPa driving pressure was applied, a GeneRuler^{TM} 1-kbp Plus DNA Ladder was separated within 5 minutes.

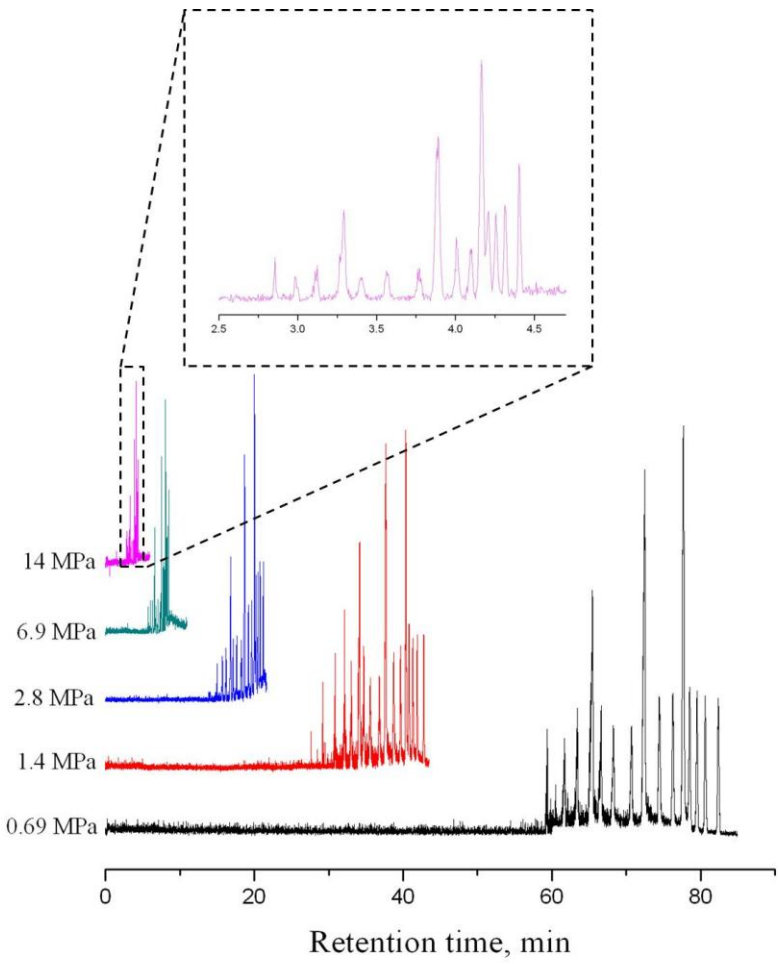

Figure 4.8. Chromatograms obtained at different elution pressures. The separation capillary had a total length of 70 cm (65 cm effective). The injection volume was estimated to be 2.4 pL, and the elution pressure was controlled by tuning the applied voltage (550 V – 11.1 kV) to the EOP. Inset shows an expanded view of the fastest separation. All other conditions were the same as in Figure 4.5.

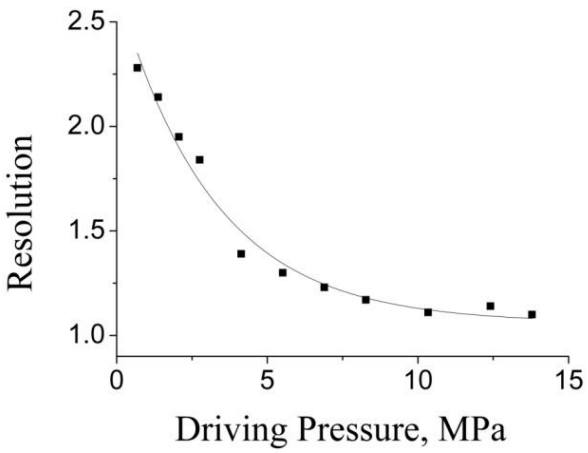

Figure 4.9. Effect of the elution pressure on resolutions. All data was obtained from Figure 4.8.

4.4 Applications

We finally applied the developed system to size plasmid DNA. The plasmid DNA was from *E-coli* (a transformant of BL21(DE3) competent cell), and it was prepared as follows: (1) E. coli was grown in 5 mL complete Luria-Bertani medium at 37^0C overnight; (2) Bacteria cells were harvested by centrifugation at 13000 rpm for 60 s; (3) A commercial kit (Qiaprep spin miniprep kit, Qiagen, Germantown, MD) was utilized to extract plasmid DNA from the cells; (4) The extracted plasmid DNA was digested with a restriction enzyme, XbaI (New England Biolabs, Ipswich, MA). 10 activity units of XbaI in 20 mL reaction solution for digesting 1.2

mg plasmid DNA; (5) A commercial kit (QIAquick PCR Purification Kit, Qiagen) was finally used to purify the digested plasmid DNA. As shown in Figure 4.10A, with GeneRuler^{TM} 1-kbp Plus DNA Ladder as the sizing marker, the linear plasmid DNA was estimated to be 4.5 kbp, which was close to the theoretical value (4.46 kbp). In the middle trace (trace *b*), multiple peaks were observed. This may be due to the conformation of supercoiled and open circular plasmid. The same three samples were also analyzed with agarose gel electrophoresis. As shown in Figure 2.10B, the resolutions in agarose gel electrophoresis were comparable to those in BaNC-HDC. However, in BaNC-HDC, the separation time was shortened from 45 to 5 minutes and the required DNA sample was minimized to 10 pg. Additionally, separation efficiencies in BaNC-HDC were much higher than those in agarose gel electrophoresis.

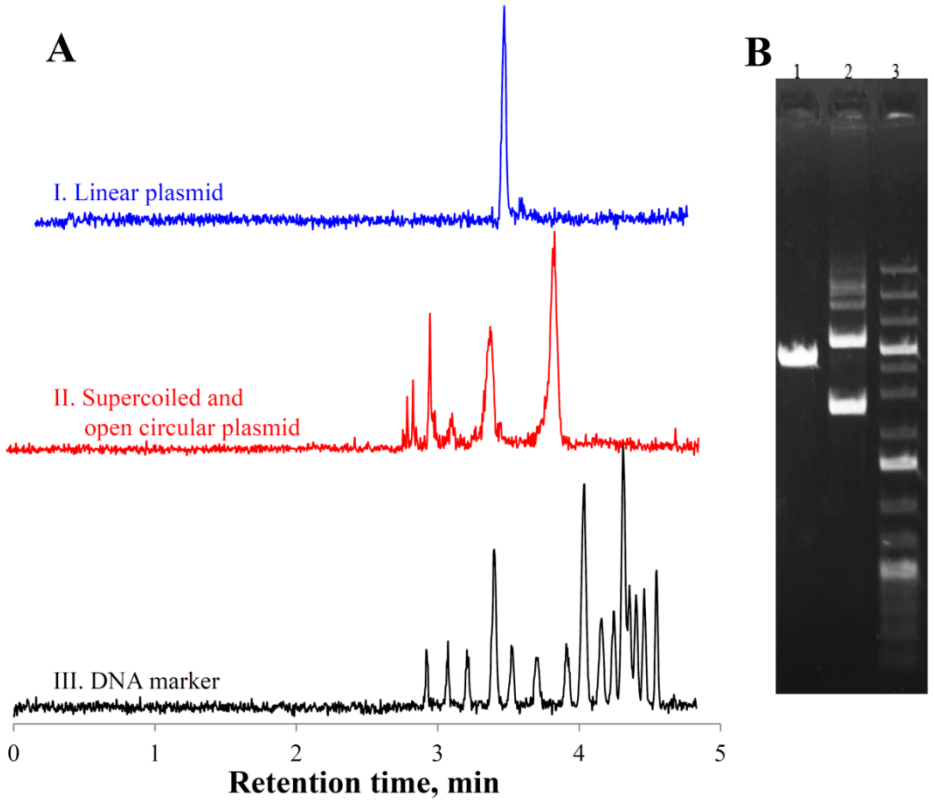

Figure 4.10. Sizing plasmid DNA with BaNC-HDC. A) Chromatograms of I) the linear plasmid DNA (3 ng/μL) after XbaI digestion, II) the supercoiled, open circular, and multimer DNA (7 ng/μL in total) before the digestion, and III) DNA size marker (20 ng/μL in total). The estimated injection volume was 2.4 pL, and the elution pressure was 13.8 MPa. All other conditions were as in Figure 4.5. B) Agarose gel electrophoresis results for the samples, with Lane 1, 2, and 3 corresponding to Trace I, II, and, respectively. The electrophoretic separation was performed using Owl* EasyCast* B2 Mini Gel Electrophoresis Systems (Thermo Scientific, Waltham, MA) at 120 volts for 45 min. The gel contained 0.7% agarose. 2

mL of 60 ng/μL linear plasmid was loaded in Lane 1, 1 mL of 150 ng/μL plasmid DNA before digestion was loaded in Lane 2, and 0.3 mL of 500 ng/μL DNA size markers was loaded in Lane 3.

4.5 Concluding remarks

In this work, we successfully incorporated an EOP and a microchip injector into the BaNC-HDC system for non-gel DNA separations. At 13.8-MPa elution pressure provided by the EOP, GeneRuler^{TM}1-kbp Plus DNA Ladder was separated within 5 minutes. With an on-chip cross and an off-chip six-port valve, the developed microchip injector could be handily operated and the injected volume was accurately controlled at picoliter level. More importantly, all major components of the apparatus, including the EOP, the microchip injector, and the separation column, can potentially be fabricated on a single LOC device to automate operations and to improve reproducibility. Integration of an EOP and a microchip injector into the BaNC-HDC system is a critical step toward developing a portable and automatic DNA analyzer for non-gel DNA analysis.

The materials in Chapter 4 are adapted from Zhu et al. Angewandte Chemie International Edition 52 (2013) 5612 –5616. The copyright was obtained from Wiley (license number: 3365990514777).

Chapter 5: High-Throughput Sizing and Quantitating DNA at the Single-Molecule Level without Sieving Matrix

5.1 Introduction

Miniaturization in analytical instrumentation can save housing space, shorten analysis time, and accordingly reduce cost requirements.[18,21,114,115] More importantly, shrunken analytical devices can be conveniently handled, and this makes it possible to perform analysis in sample locations, which is often necessary in environmental analysis and point-of-care analysis.[116,117]

Instrument miniaturization is usually accompanied by decrease in the injected sample volume,[118,119] and the required sample volume for miniature analysis can be down to picoliter level,[120,121] which make injection challenging. Our group recently proposed a novel approach, namely Bare Narrow Capillary Hydrodynamic Chromatography (BaNC-HDC), for DNA analysis in free solutions.[8,11,110] This technique is performed in a bare capillary of 1-10 μm i.d. and the required sample volume ranges from 1 to 100 pL. Originally, DNA samples were bomb loaded, and the injection was too complicated to be precisely controlled. Later, to automate the separation system and improve injection reproducibility, we incorporated a microchip injector into the BaNC-HDC system to inject picoliters of samples.[53] With the proposed injection scheme, DNA samples were reliably and

reproducibly injected into the separation column at picoliters (down to 1.2 pL). However, injection and separation were still isolated and, as a result, continuous DNA separations in BaNC-HDC were not feasible. Herein, we aimed to developing an easy-to-be-controlled injector which is capable of delivering subpicoliters of samples for continuous DNA separations in BaNC-HDC.

Currently, a number of methods exist for sample injections at picoliter level,[121-125] and most of these methods are driven by electrical field.[122-124] The electrically driven injections are based on electroosmotic flow or electrophoretic immigration, and the injected amount of samples is controlled by tuning the applied electrical field and the injection time. These methods can be used to precisely introduce hundreds of picoliters of samples, but no reports were found to inject samples at the level of subpicoliters. Additionally, BaNC-HDC is driven by pressure,[8,9] and applying high voltage for injections will complicate the system, restricting the applications of BaNC-HDC. As mentioned above, when DNA samples were bomb loaded[8,9] or loaded with the previously developed injector,[53] injection and separation were two isolated steps, and this not only brought about complicated operations but also made successive DNA separations impossible. In this work, we incorporated a commercial 60-nL injector into the BaNC-HDC system and, between the injector and the separation column,

an on-chip cross was used to split a slight portion of the injected samples into the separation column while most of the samples were flushed away. This injection scheme allowed injecting samples at subpicoliter level. More importantly, with this injection scheme, injections could be performed while separations were in process, which made successive DNA separations feasible and greatly improved throughput of BaNC-HDC. To demonstrate the applicability of the developed system, we finally utilized it to size digested λ-DNA and identify budding yeast strains. The developed system was capable of handling real-world samples not requiring any further purification.

5.2 Experimental section

5.2.1 Reagents and materials

Fused-silica capillaries were products of Polymicro Technologies (Phoenix, AZ). GeneRuler^{TM} 1-kbp Plus DNA Ladder (SM1331) was purchased from Fermentas Life Sciences Inc. (Glen Burnie, MD), and YOYO-1 was from Molecular Probes (Eugene, OR). Concentrated hydrochloric acid, ethylenediaminetetraacetic acid (EDTA), fluorescein, sodium hydroxide, and tris(hydroxymethyl)aminomethane (Tris) were obtained from Fisher Scientific (Fisher, PA).

5.2.2 Preparation of separation buffer and DNA samples

Preparation of separation buffer. The separation buffer, 10 mM TE, was composed of 10 mM Tris and 1.0 mM Na_2EDTA at pH 8.0. Stock solutions of 400 mM Tris and 400 mM Na_2EDTA were prepared by dissolving the appropriate amounts of chemicals in DDI water from a Nanopure^{TM} Infinity Ultrapure Water System (Barnstead, Newton, WA). pH of the stock solutions was adjusted to ~8.0 with concentrated hydrochloric acid or 1 M sodium hydroxide. 10 mM TE was prepared by mixing 400 mM Na_2EDT, 400 mM Tris, and DDI water at the ratio of 1:10:389. Before being used, all solutions were filtered through a 0.22-μm filter (VWR, TX) and vacuum-degassed.

Preparation of standard DNA samples. The stock solution of 100 ng/μL GeneRuler^{TM} 1-kbp Plus DNA Ladder was prepared by mixing 39 μL 10 mM TE buffer, 10 μL 500 ng/μL DNA, and 1 μL YOYO-1. Working standard DNA solutions were made by diluting the stock solution with the 10 mM TE buffer at the ratio as needed.

Preparation of digested λ-DNA. λ-DNA was purchased from New England Biolabs (Ipswich, MA). A restriction enzyme, *Hin*d III (New England Biolabs, Ipswich, MA), was used to digest λ-DNA; 10 activity

units of *Hin*d III for 2.5 μg lambda DNA in a 50 μL reaction at 37 ^{0}C overnight. Digested λ-DNA was used without further purification.

Preparation of budding yeast DNA. Bioethanol *S. cerevisiae* strains, CAT-1 and BG-1, were kindly supplied by Drs. Ana Teresa B. F. Antonangelo and Debora Colombi at San Paulo State University in Brazil. Strains grew in 10 mL yeast peptone dextrose (YPD) medium for 12 – 16 h at 30 ^{0}C until A_{600} of culture reached to 0.6 – 0.8. DNA of yeast cultures was extracted using Yeast Genomic DNA Purification Kit (AMRESCO, Solon, OH). The amplification of the tandem repeats marker, G4, was conducted following the method as described previously with modifications.[126] Briefly, 50 μL polymerase chain reaction (PCR) solution contained 100 ng genomic DNA, 10 μL of 5×Reaction Buffer, 800 μM dNTP mix (200 μM each), 0.2 μM of each forward and reverse primer for locus G4 (forward primer: 5´-AACCCATTGACCTCGT-TACTATCGT-3'; reverse primer: 5´-TTCGATGGCTCTGATAACTCCA-TTC-3'), 5 units of Tfi DNA polymerase (Invitrogen, Carlsbad, CA), and 1.5 mM of $MgCl_2$. PCR reaction was proceeded by denaturing at 94 ℃ for 5 min, cycling temperatures for 14 cycles from 94 ℃ for 15 s, to 60 ℃ for 30 s (this temperature was decreased by 1 ℃ for every cycle), and to 72 ℃ for 30 s, cycling temperatures for 25 cycles from 94 ℃ for 15 s, to 48 ℃ for 30 s, and to 72 ℃ for 30 s, and maintaining the temperature at 72 ℃ for 5 min. PCR

products were characterized with slab gel electrophoresis. PCR products were analyzed without any further purification.

5.2.3 Apparatus

As shown in Figure 5.1, the experimental setup used in this work was composed of a pressure chamber, a 60-nL injector (C14W. 16, VICI, Houston, TX), a microfabricated flow splitter, a bare narrow capillary, and a confocal laser-induced fluorescence (LIF) detector. The pressure chamber was in-laboratory machined and it could sustain a pressure of up to 14 MPa without leakage. The microfabricated flow splitter consisted of an on-chip cross and a commercial stream selector (C5-2006, VICI, Houston, TX). The on-chip cross was fabricated with standard photolithographic technologies as previously reported.[102,112] Briefly, a glass wafer, which was beforehand sputtered with 30 nm Cr and 500 nm Au, was annealed at 150^0C for 1.5 h. After being coated with photoresist, the glass wafer was soft-baked at 85^0C for 20 min. Then, the photoresist was exposed to UV light under the photomask, and the exposed photoresist was developed in MF^{TM}-319 (Rohm and Haas Electronic Materials LLC, Marlborough, MA). After the unveiled Cr/Au was etched off, the wafer was etched in concentrated hydrofluoric acid for ~13 min. After the Cr/Au layer was thoroughly removed, the generated grooves were roughly semicircular because the line-

width on the photomask was narrow (5 μm). Round channels were formed by face-to-face aligning and bonding two etched wafers.

The separation capillary, SC, (47-cm-long, 150-μm-o.d., and 2-μm-i.d.) and three auxiliary capillaries, AC_{1-3}, (all 6.5-cm-long, 150-μm-o.d., and 20-μm-i.d.) were glued into the on-chip cross with epoxy adhesive. AC_1 was connected to the column end of the 60-nL injector, of which the pump end was introduced to the solution vial inside the pressure chamber via another auxiliary capillary (AC_4). The other two auxiliary capillaries (AC_2 & AC_3) were connected to two ends of a micro-Tee (P-727, IDEX, Lake Forest, IL) while the third end of the Tee was led to the stream selector via an additional auxiliary capillary (AC_5). Six restriction capillaries, RC_{1-6}, were assembled into the six ports of the stream selector for controlling the flow rate through the stream selector and accordingly tuning the splitting ratio. The whole system was driven by a pressure-regulated nitrogen gas which was introduced to the pressure chamber through a capillary. This capillary and the auxiliary capillary, AC_4, were inserted into PEEK tubing and they were then anchored to the pressure chamber by screwing the PEEK tubing with high-pressure fittings (ZNF1PKG-5, VICI, Houston, TX).

The LIF detector was in-house built as previously described.[126] Briefly, a 488-nm beam from an argon ion laser (Laserphysics, Salt Lake City, UT, USA) was reflected by a dichroic mirror (Q505LP, Chroma

Technology, Rockingham, VT, USA) and focused onto the narrow capillary through an objective lens (206 and 0.5 NA, Rolyn Optics, Covina, CA, USA). Fluorescence from the narrow capillary was collimated by the same objective lens, and collected by a photosensor module (H5784-01, Hamamatsu, Japan) after passing through the dichroic mirror, an interference band-pass filter (532 nm), and a 2-mm pinhole. The output of the photosensor module was acquired with a MCC data acquisition board (USB-FS1608, Measurement Computing Corporation, Norton, MA) The data were acquired and treated with program written in-laboratory with Labview (National Instruments, Austin, TX).

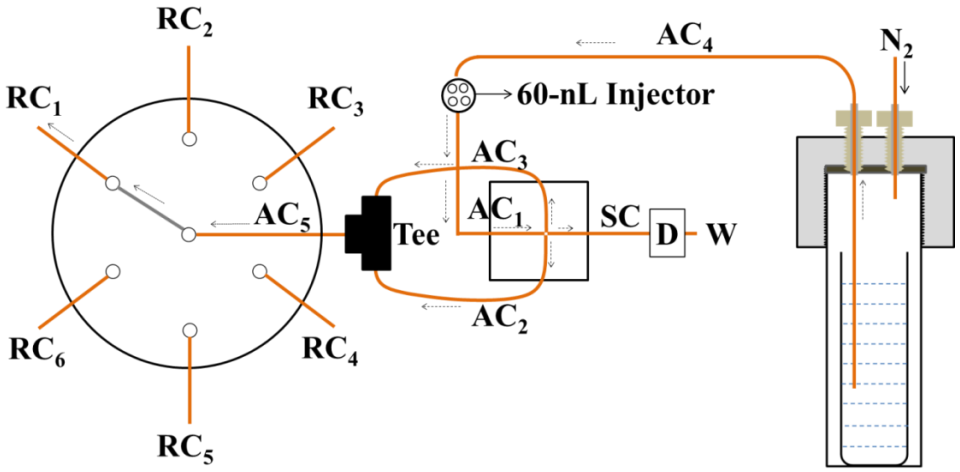

Figure 5.1. Schematic diagram of the experimental setup used for successive DNA separations in BaNC-HDC. AC_{1-5}, auxiliary capillaries; SC, separation capillary; RC_{1-6}, restriction capillaries; D, LIF detector; W,

Waste. The six-port stream selector was shown on the left while the pressure chamber was presented on the right. The six-port stream selector (C5-2006) was purchased from VICI (Houston, TX), and the pressure chamber was in-house machined with stainless steel. The separation capillary had a total length of 47 cm (41-cm effective length), an o.d. of 150 μm, and an i.d. of 2 μm. All three auxiliary capillaries attached the on-chip cross, AC_{1-3}, had a length of 6.5 cm, an o.d. of 150 μm, and an i.d. of 20 μm while the other two auxiliary capillaries, $AC_{4, 5}$, had a length of 30 cm, an o.d. of 360 μm, and an i.d. of 150 μm. RC_1 had a length of 6 cm, an o.d. of 360 μm, and an i.d. of 50 μm, relating to the splitting ratio of $0.43:6*10^4$. All other five restriction capillaries, RC_{2-6}, had an o.d. of 150 μm and an i.d. of 20 μm. The lengths of RC_{2-6} were 3.5 cm, 10 cm, 19 cm, 30 cm, and 41 cm, respectively, relating to the splitting ratios of 0.85, 1.70, 2.83, 4.25, and $5.66:6*10^4$.

5.2.4 Alignment of the detection window with LIF detector

The solution vial inside the pressure chamber was firstly loaded with ~4 mL 1 μM fluorescein. After the pressure chamber was tightly screwed, the pressure-regulated nitrogen gas was introduced into the pressure chamber to drive the fluorescein solution into the system. As the applied pressure was fixed, the fluorescein solution flowed through the separation capillary at a constant flow rate. Via the translation stage, the position of the

detection window was adjusted until the maximum signal output was obtained. The positions of the translation stage in three dimensions were then locked, and the signal output was monitored for ~30 min. If the signal output did not drift or fluctuate, the position of the detection window was considered to be aligned and settled. The separation capillary was finally flushed with the eluent (10 mM TE buffer) until the signal output dropped to the background level.

5.2.5 Measurement of splitting ratios

Splitting ratios were obtained by simultaneously measuring the flow rate in the separation capillary and that in the restriction capillary. An empty capillary with 10 μm i.d. was connected to the outlet of the separation capillary to collect the solution flowing out, and the movement of the liquid meniscus was monitored under a microscope. Flow rates were calculated using as follows

$$Q_{sc} = \frac{\pi d^2 l}{4t} \qquad (5.1)$$

where Q_{sc} is the flow rate in the separation capillary, d is the inner diameter of the collection capillary, l is the distance the liquid meniscus migrated, and t is the migration time. While the flow rate in the separation capillary was being measured, the solution coming out of the restriction capillary was

collected with a vial and weighed, and the flow rate in the restriction capillary was calculated as follows,

$$Q_{rc} = \frac{m}{\rho * t} \qquad (5.2)$$

where Q_{rc} is the flow rate in the restriction capillary, ρ is density of water, and t is the collection time. The splitting ratio was defined as the ratio of the flow rate in the separation capillary to that in the restriction capillary (Q_{sc}:Q_{rc}).

5.2.6 Successive DNA separations in BaNC-HDC

With the integrated splitter, DNA samples could be injected into the separation capillary while separations were being performed, allowing successive DNA separations in BaNC-HDC. The system was continuously run with multiple sample injections, and the next sample was injected before the peaks of the previous one appeared.

5.3 Results and discussion

With the injection scheme we previously reported,[53] the injection volume in BaNC-HDC could be precisely controlled at picoliter level. GeneRuler^{TM} 1-kbp Plus DNA Ladder could be baseline separated within 10 minutes with high resolutions while only molecules of DNA were required for each assay. However, injection and separation could not be

performed simultaneously and, as a result, successive DNA separations were not feasible in BaNC-HDC. In this project, we aimed to improving the throughput of BaNC-HDC and automating BaNC-HDC by incorporating a splitting-based microchip injector into the BaNC-HDC system.

5.3.1 Injection schemes

The commercially-available injectors are usually of nanoliters (e. g., 4 nL and 60 nL), which are much larger than the sample volume required in BaNC-HDC. Therefore, we turned to the splitting injection mode which is often utilized in gas chromatography[127,128] but not in liquid chromatography or hydrodynamic chromatography. Initially, a 4-nL injector was used while the splitting ratio was controlled at ~1:4000, and the delay time was a few seconds. In an attempt to minimizing the delay time, a 60-nL injector was used, and the delay time was shortened to <0.1 s. Meanwhile, reproducibility for peak areas was found to be improved. Therefore, a 60-nL injector was used in the following experiments.

Referring to Figure 5.1, with a commercial injector (C14W. 16, VICI, Houston, TX), 60-nL DNA sample was introduced into the BaNC-HDC system. As the sample solution passed the cross section, a slight portion (<0.01%) of the sample was split into the separation capillary while most of it was flushed away through the stream selector. The sample volume

injected into the separation capillary was determined by the splitting ratio, which was determined by the selected restriction capillary. The splitting ratio was measured as described in Section 5.2.5. The performance of the homemade splitter was first investigated with standard fluorescein solutions, and reproducibility with RSDs of ~2% was obtained. To demonstrate the improvement in throughput of BaNC-HDC and to evaluate the ability of the developed method for quantitative analysis, 30 fluorescein samples at 5 different concentrations (6 samples at each concentration) were continuously injected with the injection period of 60 s. As the fluorescein concentration increased, peak areas increased proportionally (see Figure 5.2a) with linear regression coefficient of 0.9968 (see Figure 5.2b). The calculated limit of detection (LOD) for fluorescein was 0.93 nM (S/N = 3). It should be noticed that only ~0.85 pL was actually injected into the separation capillary in each injection, meaning only ~500 molecules of fluorescein were required to be detected by the BaNC-HDC system. The linearity of the response was also established with GeneRuler^{TM} 1-kbp Plus DNA Ladder over the total concentration range of 5-100 ng/μL (see Figure 5.3a) and, for all DNA fragments, satisfactory linear relationships were achieved with linear regression coefficients ranging from 0.9749 to 0.9883 (see Figure 5.3b). However, the slope varied from one fragment to another, presumably due to bonding variations between DNA and YOYO-1.

Because DNA having similar sizes usually had similar slopes, we developed an approximate method for determining DNA quantities. For example, after we measure the peak area of a DNA fragment having a size of b bp, we first identify two calibration curves in Figure 5.3b for two fragments having sizes of a and c bp; a and c are the closest to b, but $a<b<c$. Because we know the calibration curve for the a-bp DNA is $Y=m_aX$ (where Y is the fluorescence signal and X is the DNA concentration) and the calibration curve for the c-bp DNA is $Y=m_cX$, the calibration curve for quantitating the b-bp DNA should be

$$Y = \left(\frac{b-a}{c-a}m_a + \frac{c-b}{c-a}m_c\right)X \qquad (5.1)$$

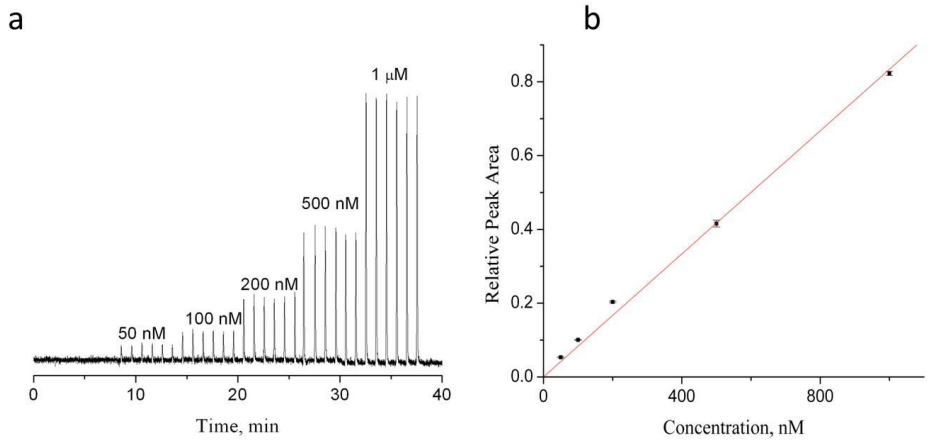

Figure 5.2. Linearity of the BaNC-HDC system for fluorescein. (a) BaNC-HDC chromatograms for successively injecting fluorescein solutions. The separation capillary had a total length of 47 cm (41 cm effective), an i.d. of 2 μm, and an o.d. of 150 μm. The eluent was 10 mM TE buffer at pH ~8, and the fluorescein solutions were prepared with the eluent. The stream selector was on RC_2 (the restriction capillary was of 3.5-cm length, 150-μm o.d., and 20-μm i.d.) position, and the measured splitting ratio was ~$0.85:6*10^4$. The injection period was 60 s. The applied pressure to the pressure chamber was 2.48 MPa. (b) Relationship between the peak area and the fluorescein concentration. Peak areas were obtained from Figure 5.2a.

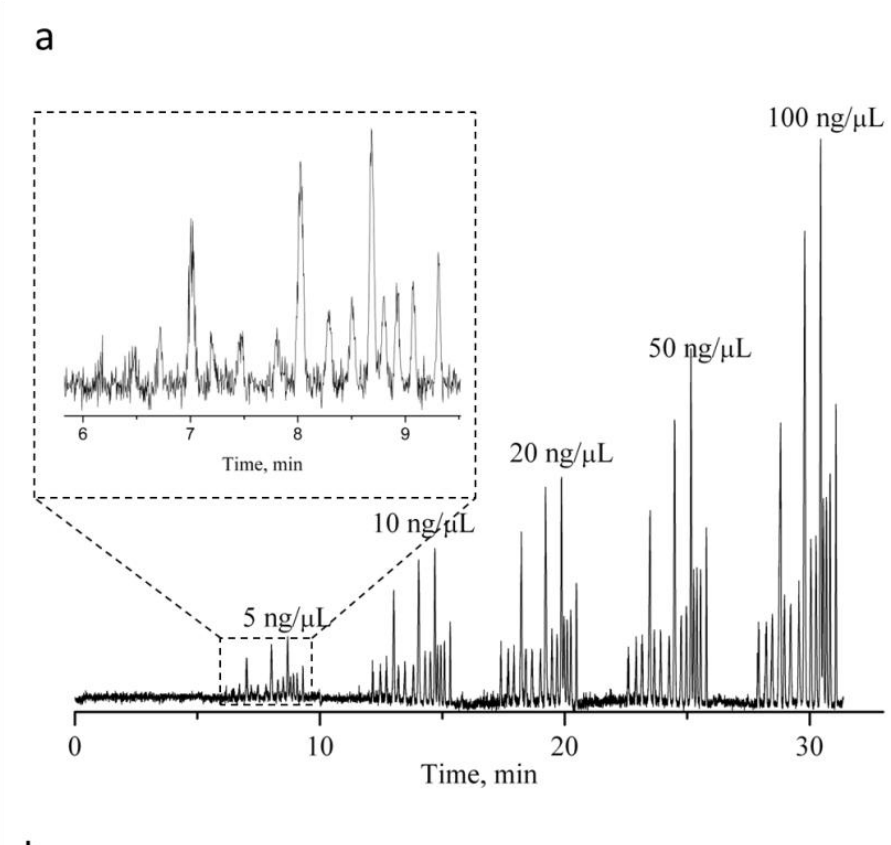
a
100 ng/μL
50 ng/μL
20 ng/μL
10 ng/μL
5 ng/μL
6
7
8
9
Time, min
0
10
20
30
Time, min
b
20 kbp
10 kbp
7 kbp
5 kbp
4 kbp
3 kbp
2 kbp
1.5 kbp
1 kbp
0.7 kbp
0.5 kbp
0.4 kbp
0.3 kbp
0.2 kbp
0.075 kbp
Relative Peak Area
0
0.2
0.4
0.6
0.8
0
5
10
15
Concentration, ng/μL

Figure 5.3. Linearity of the BaNC-HDC system for GeneRuler^{TM} 1-kbp Plus DNA Ladder. (a) BaNC-HDC chromatograms for successively injecting GeneRuler^{TM} 1-kbp Plus DNA Ladder. 100 ng/μL GeneRuler^{TM} 1-kbp Plus DNA Ladder was prepared as described above, and all working standard DNA solutions were made by diluting the 100 ng/μL stock solution with the eluent at the ratio as needed. All other conditions were as in Figure 5.2a. (b) Relationships between the peak area and the fluorescein concentration for DNA fragments. Peak areas were obtained from Figure 5.3a.

5.3.2 Splitting ratios

To investigate the reliability of the splitting-based microchip injector, splitting ratios were adjusted by changing the resistance of the restriction capillaries. As the splitting ratio decreased from $5.66:6*10^4$ to $0.85:6*10^4$, the peak height decreased accordingly (see Figure 5.4a), and good linear relationships were obtained between the peak area and the splitting ratio with linear regression coefficients in the range of 0.9941-0.9987 (see Figure 5.4b). By decreasing the splitting ratio, the sample volume injected into the separation capillary was decreased and the initial sample plug was accordingly narrowed, so resolutions were improved (see Figure 5.4a).

However, when the splitting ratio was below $0.85{:}6*10^4$, further decrease in the splitting ratio considerably decreased concentration sensitivity while resolutions were not observed to improve. To make this hypothesis straightforward, the effect of the splitting ratio on the performance of BaNC-HDC was investigated in a wider range with a mixture of four individual DNA fragments (75 bp, 1.5 kbp, 5 kbp, and 20 kbp). As shown in Figure 5.5, peak plateaus were observed when the splitting ratio was $13.90{:}6*10^4$. Decreasing the splitting ratio narrowed all peaks and improved resolutions. However, decreasing the splitting ratio below $0.87{:}6*10^4$ majorly cut down peaks while resolutions were not considerably improved. At the splitting ratio of $0.43{:}6*10^4$, the two peaks with lower concentration (20-kbp and 5-kbp, both at 0.5 ng/μL) disappeared. At the splitting ratio of $0.22{:}6*10^4$, no peaks were observed. In this work, $0.85{:}6*10^4$ was selected as a compromise between resolution and concentration sensitivity.

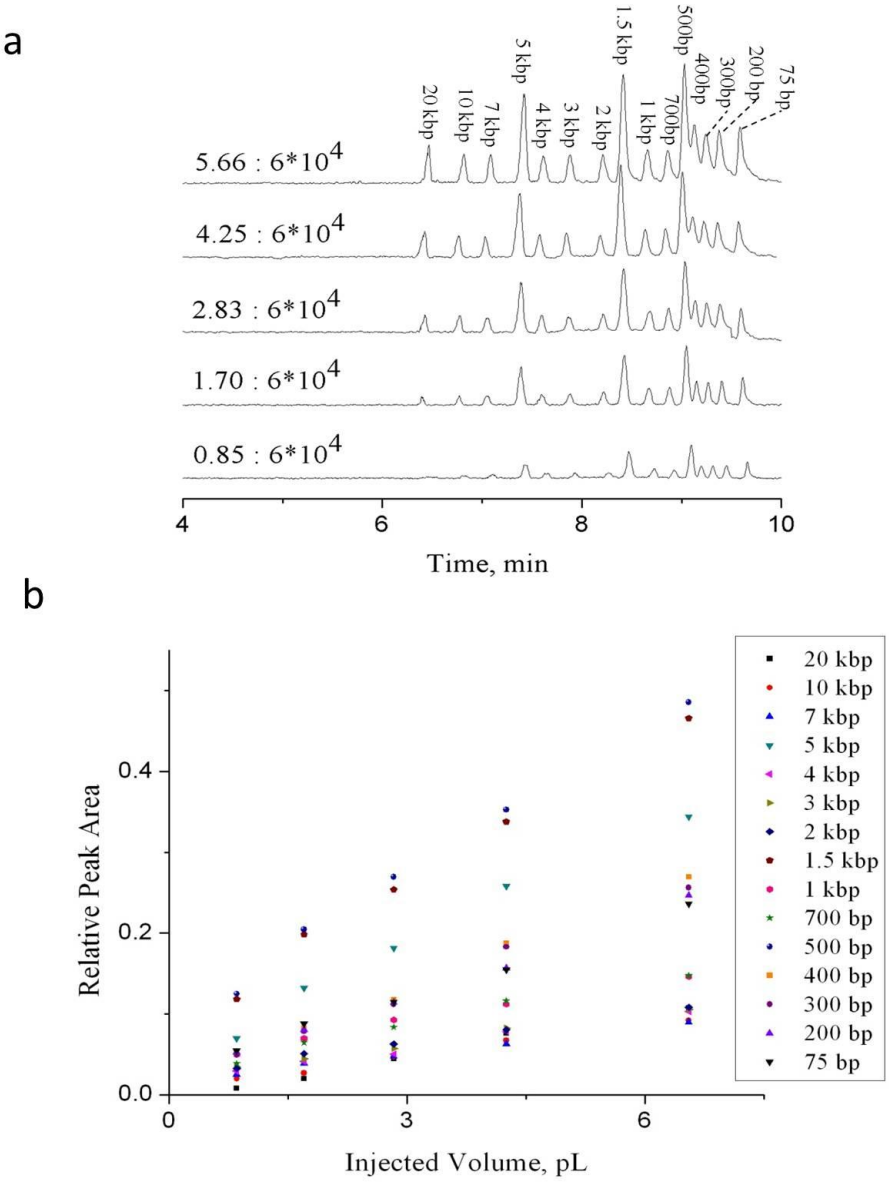

Figure 5.4. Effect of the injection volume on DNA separations in BaNC-HDC. (a) BaNC-HDC chromatograms at different splitting ratios. Sample, 10 ng/μL GeneRuler^{TM} 1-kbp Plus DNA Ladder. The splitting ratios were as shown in the figure and all other conditions were as in Figure 2a. (b)

Relationships between the peak area and the injection volume. Peak areas were obtained from Figure 5.4a.

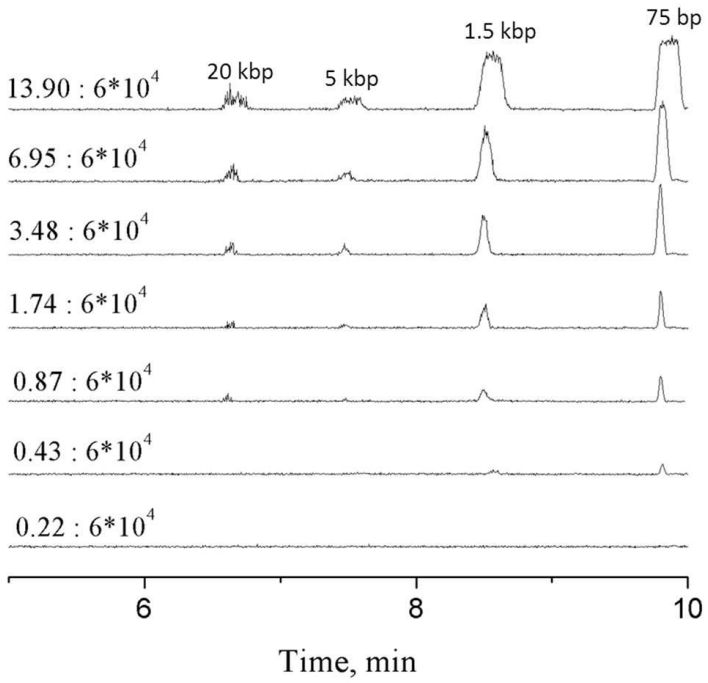

Figure 5.5. Effect of the injection volume on concentration sensitivity in BaNC-HDC. Mixture of four individual fragments. 20-kbp and 5-kbp fragments were both at 0.5 ng/μL while 1.5-kbp and 75-bp fragments were at 1.25 ng/μL. The splitting ratios were shown in the figure, and other conditions were as in Figure 5.4a.

5.4 Applications

To evaluate the applicability of BaNC-HDC, the developed system was utilized to analyze λ-DNA digested by *Hin*d III. As shown in Figure 5.6a, all six fragments could be identified within 10 min although 2.0-kbp and 2.3-kbp fragments were not baseline separated. One advantage of BaNC-HDC was that the diffusion coefficients of DNA fragments in the confined environment were significantly reduced[103,129,130] and, as a result, the band-broadening caused by diffusion was negligible. Therefore, resolution could be improved by decreasing the elution pressure.[52] Herein, we decreased the applied pressure from 2.48 psi to 1.24 MPa, and 2.0-kbp and 2.3-kbp fragments were successfully resolved (see Figure 5.7). The only expense was that the analysis time was lengthened to ~17 min. However, compared with the time consumed in agarose gel electrophoresis (usually 1.5 – 3 hours), BaNC-HDC was still a more time-effective method for DNA separations.

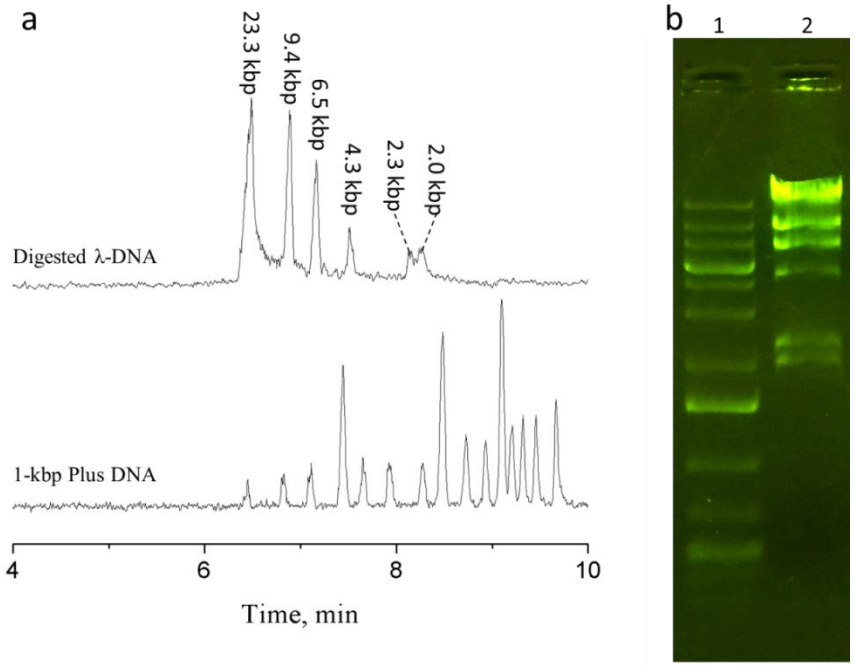

Figure 5.6. Analysis of λ-DNA digested by *Hin*d III with BaNC-HDC. (a) Chromatograms of GeneRuler^{TM} 1-kbp Plus DNA Ladder (the under trace) and λ-DNA digested by *Hin*d III (the upper trace). GeneRuler^{TM} 1-kbp Plus DNA Ladder, 10 ng/μL; digested λ-DNA, 5 ng/μL. All other conditions were as in Figure 5.2a. (b) Agarose gel electrophoresis results. Lane 1, 0.3 μL 500-ng/μL GeneRuler^{TM} 1-kbp Plus DNA Ladder; Lane 2, 1.3 μL 50-ng/μL digested λ-DNA; The electrophoretic separation was performed using Owl*EasyCast* B2 Mini Gel Electrophoresis Systems (Thermo Scientific, Waltham, MA) at 120 volts for 45 min. The gel contained 0.8% agarose.

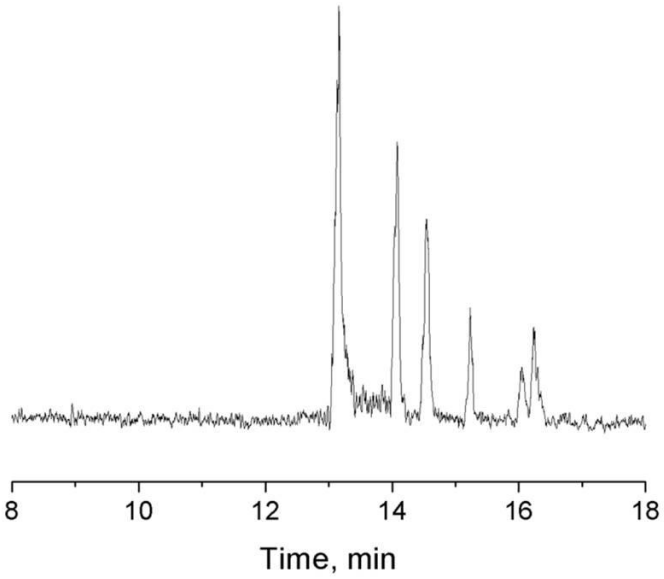

Figure 5.7. Baseline separation of digested λ-DNA. The applied pressure was 400 psi, and all other conditions were as in Figure 5.6a.

To demonstrate the applicability of BaNC-HDC to analyze real samples, we also utilized the developed system to identify yeast strains with tandem repeats as markers. Tandem repeats, also named microsatellites, are short repeat DNA sequences adjacent to each other. They are widespread and highly dynamic in both prokaryotic and eukaryotic genomes, from bacteria to human.[131] Tandem repeats are involved in complex evolution and play an important role in genomic organization and gene regulation.[132,133] In human, tandem repeats are associated with disease such as cancers and neurodegenerative disorder including Huntington's disease

and fragile X syndrome.[134] Therefore, they are widely used as markers for analysis of genetic and population diversity and for diagnose of diseases. Recently, with tandem repeats as markers, Antonangelo et al.[126] used 11 loci to investigate the genetic diversity of *S. cerevisiae* yeast strains, revealing the yeast population structure in Brazil. In this work, as demonstrations, we used locus G4 to identify two yeast strains, BG-1 and CAT-1. As shown in Figure 5.8a, with BaNC-HDC, tandem repeats were resolved and distinguished within 10 minutes while 1.5 – 3 hours were consumed in agarose gel electrophoresis (Figure 5.8b). This meant the developed system could serve as a simple and rapid tool for species identification and clinical diagnosis.

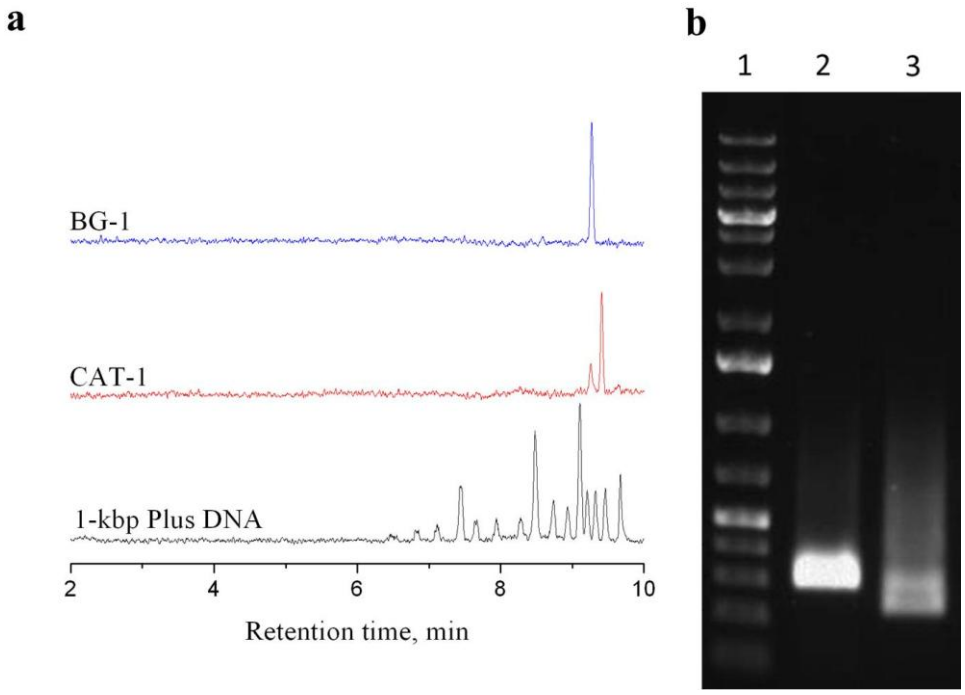

Figure 5.8. Investigating the genetic diversity of *S. cerevisiae* using BaNC-HDC with tandem repeats as markers. (a) Chromatograms of GeneRuler^{TM} 1-kbp Plus DNA Ladder, tandem repeats from BG-1, and tandem repeats from CAT-1. GeneRuler^{TM} 1-kbp Plus DNA Ladder, 10 ng/μL; tandem repeats from yeast strains were both of ~2.5 ng/μL. All other conditions were as in Figure 5.2a. (a) Characterization of DNA tandem repeats by agarose gel electrophoresis. The electrophoretic separation was performed using Wide Mini-Sub Cell GT Cell (Bio-Red, Hercules, CA) at 80 volts for 90 min. The gel contained 0.8% agarose. Lane 1: 3 μL of 50-ng/μL GeneRuler^{TM}1-kbp plus DNA Ladder; Lane 2: 10 μL of ~50 ng/μL locus G4 BG-1; Lane 3: 10 μL of ~10 ng/μL locus G4 CAT-1.

To validate the method for measuring the lengths of DNA fragments, we use the bottom chromatogram in Figure 5.8a to establish a relationship between the relative mobility of a DNA and its length based on an HDC quadratic model as we described previously.[11] Relative mobility was defined as the ratio of the velocity of a DNA fragment to the average velocity of the eluent. The fragment velocity was calculated by dividing the effective capillary length by its retention time, while the eluent velocity was obtained by measuring its flow rate and dividing the measured flow rate by the narrow capillary cross-section area. As presented in Figure 5.9, the curve-fitting generated an excellent correlation coefficient (R^2=0.9997).

$$Y_i = 1 + 2 * \left(81 * \frac{{L_i}^{0.65}}{R}\right) - \left(81 * \frac{{L_i}^{0.65}}{R}\right)^2 - 0.0132 * L_i \qquad (5.2)$$

where Y_i is the relative mobility of DNA fragment i ($Y_i = v_i/v_0$, where v_0 and v_i are the transport velocities of the eluent and DNA fragment i), L_i is the length of the fragment in kbp, and R is the radius of the bore of the narrow capillary. We then measured the Y_i values for the fragments in all consecutively injected samples, substituted the Y_i values into Equation 5.2, and computed the L_i. These results are listed in Table 5.1; excellent length accuracies (with single digit percentage error) were obtained.

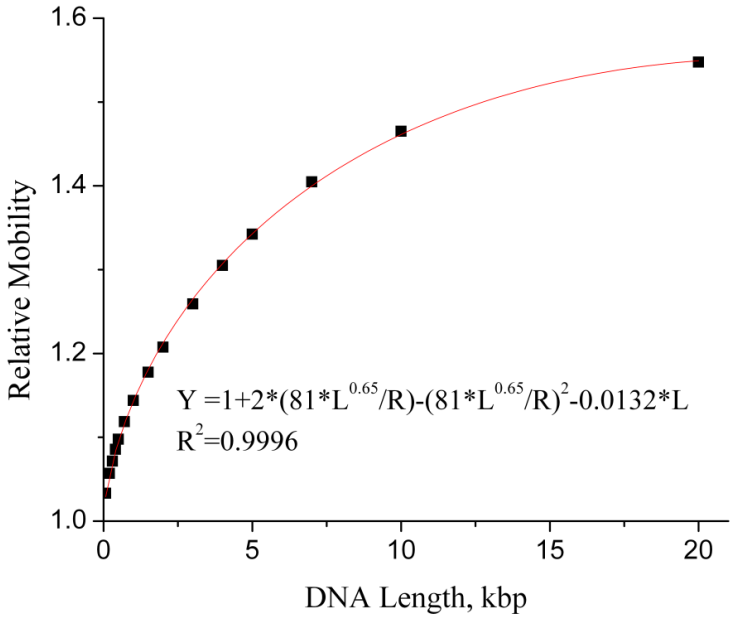

Figure 5.9 Curve-fitting results between DNA relative mobility and fragment length.

To validate the method for quantitating DNA, we measured the peak areas for all peaks in Figure 5.6a and Figure 5.8a, calculated the DNA concentrations in original samples based on the calibration curves in Figure 5.3b, and computed the number of molecules in all peaks using these calibration curves. These results are also presented in Table 5.1. There were only hundreds to thousands of DNA molecules in each peak. In general, the relative quantitation errors were around or less than 10%.

Table 5.1 DNA length and quantity measurement results.

Sample	Length, kbp		Con., ng/μL		Molecule #, 10^3	
	Actual	Measured	Actual	Measured	Actual	Measured
Digested λ-DNA	23.13	22 ± 2	4.8	5.1 ± 0.2	1.6	1.8 ± 0.1
	9.42	9.47 ± 0.04	1.9	2.2 ± 0.1	1.6	1.9 ± 0.1
	6.56	6.76 ± 0.01	1.4	1.6 ± 0.1	1.6	1.9 ± 0.1
	4.36	4.57 ± 0.03	0.90	0.71 ± 0.05	1.6	1.3 ± 0.1
	2.32	2.20 ± 0.02	0.48	0.44 ± 0.03	1.6	1.5 ± 0.1
	2.03	1.96 ± 0.03	0.42	0.39 ± 0.03	1.6	1.5 ± 0.1
Tandem Repeats	0.2 – 0.3	0.27 ± 0.02	n.a.[c]	0.13 ± 0.04	n.a.	16 ± 1
	0.3 – 0.4	0.39 ± 0.02	n.a.	0.55 ± 0.06	n.a.	4 ± 1
	0.3 – 0.4	0.38 ± 0.01	n.a.	0.76 ± 0.07	n.a.	11 ± 1

5.5 Concluding remarks

In this work, we developed a splitting-based microchip injector for successive DNA separations in BaNC-HDC. With a six-port stream selector assembled into the splitter, the splitting ratio could be handily adjusted. The constructed splitter was capable of delivering samples at subpicoliter level. Most importantly, with the splitting-based injector, injections could be performed while separations were in progress, making successive DNA separations feasible in BaNC-HDC and consequently improving the throughput of BaNC-HDC. The ultimate goal is to develop a portable, automatic, and high-throughput DNA analyzer and the developed analyzer

should find applications in remote assays, point-of-care analysis, and clinical diagnose.

The materials in Chapter 5 are adapted from a manuscript which is currently under review for publication in Analytical Chemistry.

Chapter 6: Overall Summary and Future Directions

6.1 Overall summary

This dissertation was devoted to developing a miniature and automatic BaNC-HDC system for DNA separations without using any sieving matrix. First, a new hybrid EOP was developed. In this new EOP configuration, one basic EOP unit was composed of a +EOP and a -EOP. In practice, high voltage was applied the junction of +EOP and –EOP while both the inlet and outlet of the EOP unit were grounded. With this new design, EOP units could be connected in series without short circuits and the pressure output was proportional to the number of EOP units connected. A 10-unit open-capillary EOP was capable of generating a maximum pressure 21.4 MPa. To evaluate the performance of the constructed 10-unit EOP, a micro-HPLC was built in-laboratory and it was successfully applied to separations of peptides or proteins.

We then explored the resolving power of BaNC-HDC and presented its high efficiency on separating DNA fragments. To reliably and reproducibly inject picoliters of samples in BaNC-HDC, a microchip injector was developed. With this injector, DNA samples could be accurately injected at the picoliter level while relative standard deviations for peak areas were below 5%. By integrating this chip injector and the

developed EOP into the BaNC-HDC system, the separation of GeneRuler^{TM} 1-kbp Plus DNA Ladder was accomplished within five minutes and only molecules of DNA were required for each assay. With the integrated system, plasmid DNA was accurately sized.

Later, to improve throughput of BaNC-HDC, a splitting-based injector was developed and throughput was improved from 6 to 15 assays per hour. The efficiency and resolving power of BaNC-HDC were also investigated. Under the optimized conditions, GeneRuler^{TM} 1-kbp Plus DNA Ladder was resolved with efficiencies of more than one million theoretical plates per meter. The integrated system was finally applied to analysis of plasmid DNA, digested λ-DNA, and short tandem repeats.

6.2 Future directions

The systems developed in this dissertation were majorly based on capillaries, and future work should be focused on integrating them on lab-on-a-chip devices.

High-pressure open-channel on-chip EOP was recently reported by our group, and the constructed 4-unit EOP was able to generate a pressure of up to 17 MPa.[135] Future work will include developing a battery-powered EOP to drive the BaNC-HDC system and programing all operations in BaNC-HDC. The ultimate goal is to develop a portable, automatic, and

high-throughput DNA analyzer. We expect the developed DNA analyzer to find applications in remote assays, point-of-care analysis, and clinical diagnose.

References

(1) Dimarzio, E. A.; Guttman, C. M. *Journal of Polymer Science Part B-Polymer Letters* **1969**, *7*, 267-272.

(2) Small, H. *Journal of Colloid and Interface Science* **1974**, *48*, 147-161.

(3) Tijssen, R.; Bos, J.; Van Kreveld, M. E. *Analytical Chemistry* **1986**, *58*, 3036-3044.

(4) Stegeman, G.; Kraak, J. C.; Poppe, H. *Journal of Chromatography A* **1991**, *550*, 721-739.

(5) Klavons, J. A.; Dintzis, F. R.; Millard, M. M. *Cereal Chemistry* **1997**, *74*, 832-836.

(6) Brewer, A. K.; Striegel, A. M. *Journal of Separation Science* **2010**, *33*, 3555-3563.

(7) Wang, X.; Kang, J.; Wang, S.; Lu, J. J.; Liu, S. *Journal of Chromatography A* **2008**, *1200*, 108-113.

(8) Wang, X.; Wang, S.; Veerappan, V.; Byun, C. K.; Nguyen, H.; Gendhar, B.; Allen, R. D.; Liu, S. *Analytical Chemistry* **2008**, *80*, 5583-5589.

(9) Wang, X.; Veerappan, V.; Cheng, C.; Jiang, X.; Allen, R. D.; Dasgupta, P. K.; Liu, S. *Journal of the American Chemical Society* **2010**, *132*, 40-41.

(10) Liu, K. J.; Rane, T. D.; Zhang, Y.; Wang, T.-H. *Journal of the American Chemical Society* **2011**, *133*, 6898-6901.

(11) Wang, X.; Liu, L.; Pu, Q.; Zhu, Z.; Guo, G.; Zhong, H.; Liu, S. *Journal of the American Chemical Society* **2012**, *134*, 7400-7405.

(12) Bos, J.; Tijssen, R.; Van Kreveld, M. E. *Analytical Chemistry* **1989**, *61*, 1318-1321.

(13) Ramsey, R. S.; Ramsey, J. M. *Analytical Chemistry* **1997**, *69*, 1174-1178.

(14) Lazar, I. M.; Karger, B. L. *Analytical Chemistry* **2002**, *74*, 6259-6268.

(15) Pu, Q.; Liu, S. *Analytica Chimica Acta* **2004**, *511*, 105-112.

(16) Byun, C. K.; Wang, X.; Pu, Q.; Liu, S. *Analytical Chemistry* **2007**, *79*, 3862-3866.

(17) Takamura, Y.; Onoda, H.; Inokuchi, H.; Adachi, S.; Oki, A.; Horiike, Y. *Electrophoresis* **2003**, *24*, 185-192.

(18) He, C.; Lu, J. J.; Jia, Z.; Wang, W.; Wang, X.; Dasgupta, P. K.; Liu, S. *Analytical Chemistry* **2011**, *83*, 2430-2433.

(19) Pretorius, V.; Hopkins, B. J.; Schieke, J. D. *Journal of Chromatography A* **1974**, *99*, 23-30.

(20) Yao, S.; Santiago, J. G. *Journal of Colloid and Interface Science* **2003**, *268*, 133-142.

(21) Gu, C.; Jia, Z.; Zhu, Z.; He, C.; Wang, W.; Morgan, A.; Lu, J. J.; Liu, S. *Analytical Chemistry* **2012**, *84*, 9609-9614.

(22) Shin, W.; Lee, J. M.; Nagarale, R. K.; Shin, S. J.; Heller, A. *Journal of the American Chemical Society* **2011**, *133*, 2374-2377.

(23) Serwer, P. *Electrophoresis* **1983**, *4*, 375-382.

(24) McMaster, G. K.; Carmichael, G. G. *Proceedings of the National Academy of Sciences of the United States of America* **1977**, *74*, 4835-4838.

(25) Calladine, C. R.; Collis, C. M.; Drew, H. R.; Mott, M. R. *Journal of Molecular Biology* **1991**, *221*, 981-1005.

(26) Jeppsson, J. O.; Laurell, C. B.; Franzen, B.; Alper, C. A.; Forman, D. T.; Tucker, E. S.; Ward, A. M. *Clinical Chemistry* **1979**, *25*, 629-638.

(27) Smith, C. L.; Klco, S. R.; Cantor, C. R. *Genome analysis: a practical approach*, 1988; pp 41-72.

(28) Cantor, C. R.; Smith, C. L.; Mathew, M. K. *Annual Review of Biophysics and Biophysical Chemistry* **1988**, *17*, 287-304.

(29) Schwartz, D. C.; Cantor, C. R. *Cell* **1984**, *37*, 67-75.

(30) Cohen, A. S.; Karger, B. L. *Journal of Chromatography* **1987**, *397*, 409-417.

(31) Guttman, A.; Cohen, A. S.; Heiger, D. N.; Karger, B. L. *Analytical Chemistry* **1990**, *62*, 137-141.

(32) Baba, Y.; Matsuura, T.; Wakamoto, K.; Morita, Y.; Nishitsu, Y.; Tsuhako, M. *Analytical Chemistry* **1992**, *64*, 1221-1225.

(33) Cohen, A. S.; Najarian, D. R.; Paulus, A.; Guttman, A.; Smith, J. A.; Karger, B. L. *Proceedings of the National Academy of Sciences of the United States of America* **1988**, *85*, 9660-9663.

(34) Ganzler, K.; Greve, K. S.; Cohen, A. S.; Karger, B. L.; Guttman, A.; Cooke, N. C. *Analytical Chemistry* **1992**, *64*, 2665-2671.

(35) Mansfield, E. S.; Vainer, M.; Enad, S.; Barker, D. L.; Harris, D.; Rappaport, E.; Fortina, P. *Genome Research* **1996**, *6*, 893-903.

(36) Mansfield, E. S.; Vainer, M.; Harris, D. W.; Gasparini, P.; Estivill, X.; Surrey, S.; Fortina, P. *Journal of Chromatography A* **1997**, *781*, 295-305.

(37) Gao, Q.; Pang, H.-m.; Yeung, E. S. *Electrophoresis* **1999**, *20*, 1518-1526.

(38) Pang, H.-m.; Pavski, V.; Yeung, E. S. *Journal of Biochemical and Biophysical Methods* **1999**, *41*, 121-132.

(39) Effenhauser, C. S.; Paulus, A.; Manz, A.; Widmer, H. M. *Analytical Chemistry* **1994**, *66*, 2949-2953.

(40) Woolley, A. T.; Mathies, R. A. *Proceedings of the National Academy of Sciences of the United States of America* **1994**, *91*, 11348-11352.

(41) Woolley, A. T.; Mathies, R. A. *Analytical Chemistry* **1995**, *67*, 3676-3680.

(42) Liu, S.; Shi, Y.; Ja, W. W.; Mathies, R. A. *Analytical Chemistry* **1998**, *71*, 566-573.

(43) Liu, S. R.; Ren, H. J.; Gao, Q. F.; Roach, D. J.; Loder, R. T.; Armstrong, T. M.; Mao, Q. L.; Blaga, I.; Barker, D. L.; Jovanovich, S. B. *Proceedings of the National Academy of Sciences of the United States of America* **2000**, *97*, 5369-5374.

(44) Voelkel, A. R.; Noolandi, J. *Macromolecules* **1995**, *28*, 8182-8189.

(45) Heller, C.; Slater, G. W.; Mayer, P.; Dovichi, N.; Pinto, D.; Viovy, J.-L.; Drouin, G. *Journal of Chromatography A* **1998**, *806*, 113-121.

(46) McCormick, L. C.; Slater, G. W. *Electrophoresis* **2006**, *27*, 1693-1701.

(47) Xiao, W. Z.; Oefner, P. J. *Human Mutation* **2001**, *17*, 439-474.

(48) Huang, L. R.; Tegenfeldt, J. O.; Kraeft, J. J.; Sturm, J. C.; Austin, R. H.; Cox, E. C. *Nature Biotechnology* **2002**, *20*, 1048-1051.

(49) Han, J.; Turner, S. W.; Craighead, H. G. *Physical Review Letters* **1999**, *83*, 1688-1691.

(50) Zheng, J.; Yeung, E. S. *Analytical Chemistry* **2002**, *74*, 4536-4547.

(51) Wang, X.; Cheng, C.; Wang, S.; Zhao, M.; Dasgupta, P. K.; Liu, S. *Analytical Chemistry* **2009**, *81*, 7428-7435.

(52) Zhu, Z. F.; Liu, L.; Wang, W.; Lu, J. J.; Wang, X. Y.; Liu, S. R. *Chemical Communications* **2013**, *49*, 2897-2899.

(53) Zhu, Z.; Chen, H.; Wang, W.; Morgan, A.; Gu, C.; He, C.; Lu, J. J.; Liu, S. *Angewandte Chemie International Edition* **2013**, *52*, 5612-5616.

(54) Laser, D. J.; Santiago, J. G. *Journal of Micromechanics and Microengineering* **2004**, *14*, R35-R64.

(55) Wang, X.; Cheng, C.; Wang, S.; Liu, S. *Microfluidics and Nanofluidics* **2009**, *6*, 145-162.

(56) Wang, X.; Wang, S.; Gendhar, B.; Cheng, C.; Byun, C. K.; Li, G.; Zhao, M.; Liu, S. *TrAC Trends in Analytical Chemistry* **2009**, *28*, 64-74.

(57) Paul, P. H.; Rakestraw, D. J. **2000**, U.S. Patent 6,019,882.

(58) Nie, F.-Q.; Macka, M.; Barron, L.; Connolly, D.; Kent, N.; Paull, B. *Analyst* **2007**, *132*, 417-424.

(59) Dasgupta, P. K.; Liu, S. *Analytical Chemistry* **1994**, *66*, 3060-3065.

(60) Dasgupta, P. K.; Liu, S. *Analytical Chemistry* **1994**, *66*, 1792-1798.

(61) Liu, S.; Dasgupta, P. K. *Talanta* **1994**, *41*, 1903-1910.

(62) Liu, S.; Dasgupta, P. K. *Analytica Chimica Acta* **1995**, *308*, 281-285.

(63) McKnight, T. E.; Culbertson, C. T.; Jacobson, S. C.; Ramsey, J. M. *Analytical Chemistry* **2001**, *73*, 4045-4049.

(64) Lin, J.; Lin, J.; Lin, X.; Wu, X.; Xie, Z. *Electrophoresis* **2010**, *31*, 1674-1680.

(65) Thorne, H. V. *Journal of Molecular Biology* **1967**, *24*, 203-211.

(66) Takahashi, M.; Ogino, T.; Baba, K. *Biochimica et Biophysica Acta (BBA) - Nucleic Acids and Protein Synthesis* **1969**, *174*, 183-187.

(67) Morimatsu, K.; Horii, T. *Advances in Biophysics* **1995**, *31*, 23-48.

(68) Rehm, B. H. A. *Applied Microbiology and Biotechnology* **2001**, *57*, 579-592.

(69) Tost, J.; Gut, I. G. *Journal of Mass Spectrometry* **2006**, *41*, 981-995.

(70) Aaij, C.; Borst, P. *Biochimica et Biophysica Acta (BBA) - Nucleic Acids and Protein Synthesis* **1972**, *269*, 192-200.

(71) Hayward, G. S.; Smith, M. G. *Journal of Molecular Biology* **1972**, *63*, 383-395.

(72) Djouadi, Z.; Bottani, S.; Duval, M. A.; Siebert, R.; Tricoire, H.; Valentin, L. *Electrophoresis* **2001**, *22*, 3527-3532.

(73) Viovy, J. L. *Reviews of Modern Physics* **2000**, *72*, 813-872.

(74) Wagner, L.; Lai, E. *Electrophoresis* **1994**, *15*, 1078-1083.

(75) Jung, H. J.; Bae, Y. C. *Journal of Chromatography A* **2002**, *967*, 279-287.

(76) Brownlee, R. G.; Sunzeri, F. J.; Busch, M. P. *Journal of Chromatography B: Biomedical Sciences and Applications* **1990**, *533*, 87-96.

(77) Goodwin, P. M.; Johnson, M. E.; Martin, J. C.; Ambrose, W. P.; Marrone, B. L.; Jett, J. H.; Keller, R. A. *Nucleic Acids Research* **1993**, *21*, 803-806.

(78) Peyrin, E.; Caron, C.; Garrel, C.; Ravel, A.; Villet, A.; Grosset, C.; Favier, A. *Talanta* **2001**, *55*, 291-296.

(79) Szantai, E.; Guttman, A. *Electrophoresis* **2006**, *27*, 4896-4903.

(80) Sinville, R.; Soper, S. A. *Journal of Separation Science* **2007**, *30*, 1714-1728.

(81) Schmaizing, D.; Koutny, L.; Salas-Solano, O.; Adourian, A.; Matsudaira, P.; Ehrlich, D. *Electrophoresis* **1999**, *20*, 3066-3077.

(82) Hjerten, S. *Journal of Chromatography* **1983**, *270*, 1-6.

(83) Huang, X. C.; Quesada, M. A.; Mathies, R. A. *Analytical Chemistry* **1992**, *64*, 2149-2154.

(84) Noolandi, J. *Electrophoresis* **1992**, *13*, 394-395.

(85) Mayer, P.; Slater, G. W.; Drouin, G. *Analytical Chemistry* **1994**, *66*, 1777-1780.

(86) Ren, H.; Karger, A. E.; Oaks, F.; Menchen, S.; Slater, G. W.; Drouin, G. *Electrophoresis* **1999**, *20*, 2501-2509.

(87) Vreeland, W. N.; Meagher, R. J.; Barron, A. E. *Analytical Chemistry* **2002**, *74*, 4328-4333.

(88) Meagher, R. J.; Won, J.-I.; McCormick, L. C.; Nedelcu, S.; Bertrand, M. M.; Bertram, J. L.; Drouin, G.; Barron, A. E.; Slater, G. W. *Electophoresis* **2005**, *26*, 331-350.

(89) Lau, H. W.; Archer, L. A. *Physical Review E* **2010**, *81*, 031918.

(90) Albrecht, J. C.; Lin, J. S.; Barron, A. E. *Analytical Chemistry* **2011**, *83*, 509-515.

(91) Huber, C. G.; Oefner, P. J.; Bonn, G. K. *Analytical Chemistry* **1995**, *67*, 578-585.

(92) Dickman, M. J. *Journal of Chromatography A* **2005**, *1076*, 83-89.

(93) Kato, Y.; Sasaki, M.; Hashimoto, T.; Murotsu, T.; Fukushige, S.; Matsubara, K. *Journal of Chromatography A* **1983**, *265*, 342-346.

(94) Westman, E.; Eriksson, S.; Låås, T.; Pernemalm, P.-Å.; Sköld, S.-E. *Analytical Biochemistry* **1987**, *166*, 158-171.

(95) Yamakawa, H.; Higashino, K.-i.; Ohara, O. *Analytical Biochemistry* **1996**, *240*, 242-250.

(96) Hirabayashi, J.; Ito, N.; Noguchi, K.; Kasai, K. *Biochemistry* **1990**, *29*, 9515-9521.

(97) Peyrin, E.; Guillaume, Y. C.; Grosset, C.; Ravel, A.; Villet, A.; Garrel, C.; Alary, J.; Favier, A. *Journal of Chromatography A* **2000**, *886*, 1-7.

(98) Kasai, K.-i. *Journal of Chromatography B: Biomedical Sciences and Applications* **1993**, *618*, 203-221.

(99) Huber, C. G. *Journal of Chromatography A* **1998**, *806*, 3-30.

(100) Zheng, J.; Yeung, E. S. *Analytical Chemistry* **2003**, *75*, 3675-3680.

(101) Han, J.; Craighead, H. G. *Journal of Vacuum Science & Technology a-Vacuum Surfaces and Films* **1999**, *17*, 2142-2147.

(102) Liu, S. *Electophoresis* **2003**, *24*, 3755-3761.

(103) Ma, C.; Yeung, E. S. *Analytical Chemistry* **2010**, *82*, 654-657.

(104) Li, R.; Liu, L.; Wang, Y.; Wang, X. *Chemistry Letters* **2012**, *41*, 1506-1508.

(105) Danna, K.; Nathans, D. *Proceedings of the National Academy of Sciences of the United States of America* **1971**, *68*, 2913-2917.

(106) Schmalzing, D.; Koutny, L.; Salas-Solano, O.; Adourian, A.; Matsudaira, P.; Ehrlich, D. *Electrophoresis* **1999**, *20*, 3066-3077.

(107) Carrilho, E. *Electrophoresis* **2000**, *21*, 55-65.

(108) Buchholz, B. A.; Shi, W.; Barron, A. E. *Electrophoresis* **2002**, *23*, 1398-1409.

(109) Bonn, G.; Huber, C.; Oefner, P.; Sarasep, Inc.: 1996, p 2049-2049.

(110) Wang, X.; Veerappan, V.; Cheng, C.; Jiang, X.; Allen, R. D.; Dasgupta, P. K.; Liu, S. *J. Am. Chem. Soc.* **2009**, *132*, 40-41.

(111) Wang, X.; Liu, L.; Guo, G.; Wang, W.; Liu, S.; Pu, Q.; Dasgupta, P. K. *TrAC Trends in Analytical Chemistry* **2012**, *35*, 122-134.

(112) Liu, S.; Elkin, C.; Kapur, H. *Eelectrophoresis* **2003**, *24*, 3762-3768.

(113) He, C.; Zhu, Z.; Gu, C.; Lu, J.; Liu, S. *Journal of Chromatography A* **2012**, *1227*, 253-258.

(114) Desmet, G.; Eeltink, S. *Analytical Chemistry* **2013**, *85*, 543-556.

(115) Merkoci, A.; Kutter, J. P. *Lab on a Chip* **2012**, *12*, 1915-1916.

(116) Gervais, L.; Delamarche, E. *Lab on a Chip* **2009**, *9*, 3330-3337.

(117) Golberg, A.; Yarmush, M. L.; Konry, T. *Microchimica Acta* **2013**, *180*, 855-860.

(118) Manz, A.; Harrison, D. J.; Verpoorte, E. M. J.; Fettinger, J. C.; Paulus, A.; Lüdi, H.; Widmer, H. M. *Journal of Chromatography A* **1992**, *593*, 253-258.

(119) Jacobson, S. C.; Hergenroder, R.; Koutny, L. B.; Warmack, R. J.; Ramsey, J. M. *Analytical Chemistry* **1994**, *66*, 1107-1113.

(120) Yue, G.; Luo, Q.; Zhang, J.; Wu, S.-L.; Karger, B. L. *Analytical Chemistry* **2007**, *79*, 938-946.

(121) Zhang, T.; Fang, Q.; Du, W.-B.; Fu, J.-L. *Analytical Chemistry* **2009**, *81*, 3693-3698.

(122) Monnig, C. A.; Jorgenson, J. W. *Analytical Chemistry* **1991**, *63*, 802-807.

(123) Lemmo, A. V.; Jorgenson, J. W. *Analytical Chemistry* **1993**, *65*, 1576-1581.

(124) Tao, L.; Thompson, J. E.; Kennedy, R. T. *Analytical Chemistry* **1998**, *70*, 4015-4022.

(125) Reichmuth, D. S.; Shepodd, T. J.; Kirby, B. J. *Analytical Chemistry* **2004**, *76*, 5063-5068.

(126) Antonangelo, A. T. B. F.; Alonso, D. P.; Ribolla, P. E. M.; Colombi, D. *Yeast* **2013**, *30*, 307-317.

(127) Vazquez, M. M.; Blanco, M. E. V.; Lorenzo, S. M.; Mahia, P. L.; Fernandez, E. F.; Rodriguez, D. P. *Journal of Chromatography A* **2001**, *919*, 363-371.

(128) Bonn, J.; Redeby, J.; Roeraade, J. *Analytical Chemistry* **2009**, *81*, 5327-5332.

(129) Jendrejack, R. M.; Schwartz, D. C.; Graham, M. D.; de Pablo, J. J. *Journal of Chemical Physics* **2003**, *119*, 1165-1173.

(130) Reisner, W.; Morton, K. J.; Riehn, R.; Wang, Y. M.; Yu, Z. N.; Rosen, M.; Sturm, J. C.; Chou, S. Y.; Frey, E.; Austin, R. H. *Physical Review Letters* **2005**, *94*.

(131) Usdin, K. *Genome Research* **2008**, *18*, 1011-1019.

(132) Ellegren, H. *Nature Reviews Genetics* **2004**, *5*, 435-445.

(133) Boby, T.; Patch, A. M.; Aves, S. J. *Bioinformatics* **2005**, *21*, 811-816.

(134) Verstrepen, K. J.; Jansen, A.; Lewitter, F.; Fink, G. R. *Nature Genetics* **2005**, *37*, 986-990.

(135) Wang, W.; Gu, C.; Lynch, K. B.; Lu, J. J.; Zhang, Z.; Pu, Q.; Liu, S. *Analytical Chemistry* **2014**, *86*, 1958-1964.